ELSEVIER

Coordination Chemistry Reviews
187 (1999) 329–374

COORDINATION CHEMISTRY REVIEWS

Elucidation of inorganic reaction mechanisms through volume profile analysis

Grazyna Stochel [a,b], Rudi van Eldik [a,*]

[a] *Institute for Inorganic Chemistry, University of Erlangen–Nürnberg, Egerlandstrasse 1, 91058 Erlangen, Germany*

[b] *Department of Inorganic Chemistry, Faculty of Chemistry, Jagiellonian University, ul. Ingardena 3, 30-060 Kraków, Poland*

Received 14 August 1998; received in revised form 27 November 1998; accepted 1 December 1998

Contents

* Corresponding author. Tel.: +49-9131-85-27350; fax: +49-9131-85-27387.
E-mail address: vaneldik@anorganik.chemie.uni-erlangen.de (R. van Eldik)

0010-8545/99/$ - see front matter
PII: S0010-8545(99)00009-0

Abstract

The application of high pressure kinetic and thermodynamic techniques in mechanistic studies of chemical reactions in solution, can contribute towards the elucidation of the underlying reaction mechanisms. In this review the fundamental principles involved in the construction of reaction volume profiles and the mechanistic interpretation of the latter are presented for various types of reactions in inorganic, organometallic and bioinorganic systems. These include thermal and photo-induced ligand substitution and electron-transfer reactions, as well as processes that involve the activation of small molecules. The mechanistic insight gained through volume profile analysis for non-symmetrical reactions forms the theme of this contribution.

Keywords: Reaction mechanisms; Volume profile analysis; Ligand substitution

1. Introduction

In general the application of high pressure kinetic techniques to mechanistic studies in coordination chemistry has assisted the elucidation of the underlying reaction mechanisms. Detailed accounts on such studies dealing in general with reactions of coordination compounds in solution, have been published in recent years [1–13]. It is interesting to note that in a recent review covering the activity in this area during 1987–1996, more than 1500 new data sets for measurements of kinetic and thermodynamic properties at elevated pressure on inorganic systems were reported [5]. In the case of symmetrical chemical reactions, such as solvent and ligand exchange processes where no net chemical reaction occurs, the pressure dependence of the observed rate constant reveals unique information on the nature of the transition state [6–8]. In this particular case the overall reaction volume is zero, and reactants and products have the same partial molar volumes. This is totally different in the case of non-symmetrical chemical reactions. Here the activation and reaction volumes can be used to construct a volume profile for the reaction under study [1–13]. It is the objective of this contribution to demonstrate how additional, and in many cases important, mechanistic information can be obtained from analyses of volume profiles for various types of non-symmetrical thermal and photochemical reactions in inorganic, organometallic and bioinorganic systems. A treatment of the effect of pressure on the symmetrical chemical reactions mentioned above is given elsewhere in this issue. In some cases systems will also be discussed where only activation or reaction volume data are available, i.e. where no complete volume profile can be reported, since such data can also in many cases improve our understanding of the reaction mechanisms and or the effect of pressure on the system under investigation. Typical examples were selected from the literature during the past 10 years, and in many cases from our own contributions to this area.

2. Basic concepts and experimental techniques

The application of temperature as a physical parameter can lead to the construction of an energy profile in which changes in energy along the reaction coordinate are considered in order to understand the nature of the reaction mechanism. In this respect, it has especially been the entropy term, from application of the Eyring theory, that has been useful in revealing information on 'order' in the transition state. In a similar context, the application of pressure as a physical variable can lead to insight on volume changes associated with the chemical process, as revealed by the construction of a volume profile (see Fig. 1). This is based on the fundamental thermodynamic relationship $(\delta G/\delta P)_T = V$, from which it can be derived that $(\partial \ln K/\partial P)_T = -\Delta V/RT$ and $(\partial \ln k/\partial P)_T = -\Delta V^{\neq}/RT$, where ΔV represents the reaction volume associated with the overall reaction characterized by the equilibrium constant K, and $\Delta V^{\neq}$ represents the volume of activation for the reaction characterized by the rate constant k. Thus ΔV equals the difference between the partial molar volumes of the products and the reactants, whereas $\Delta V^{\neq}$ equals the difference in partial molar volume between the transition and reactant states. It follows that the volume profile represents partial molar volume changes associated with the chemical process along the reaction coordinate and enables us to visualize the nature of the transition state in terms of volume changes that occur on either the reactant or product species during the forward or back reaction, respectively.

In general, $\Delta V^{\neq}$ and ΔV may be considered as the sum of two major components: an intrinsic part ($\Delta V^{\neq}_{intr}$ or ΔV_{intr}), which represents the change in volume due to changes in bond lengths and angles, and a solvational part ($\Delta V^{\neq}_{solv}$ or ΔV_{solv}),

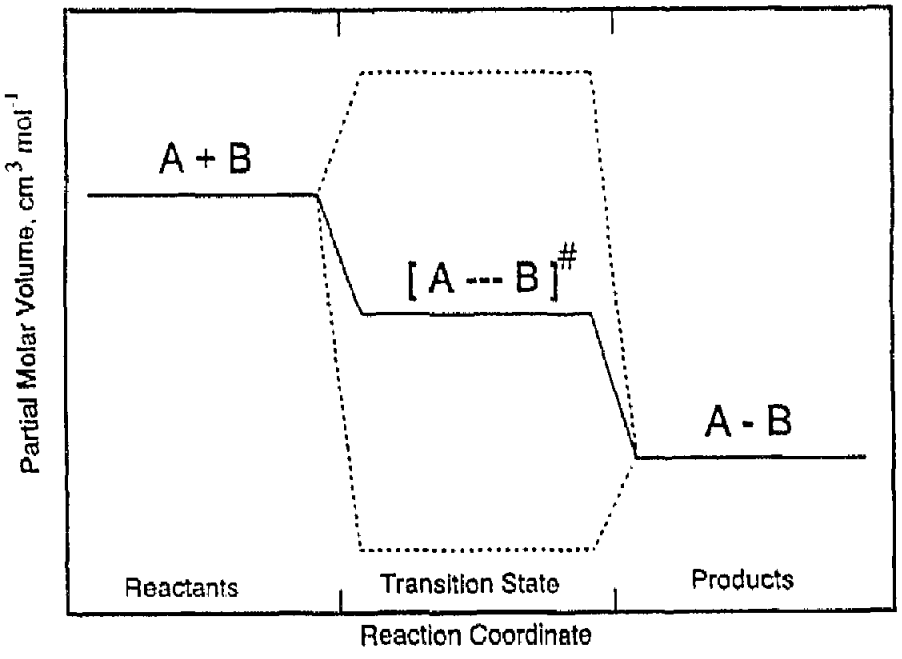

Fig. 1. Schematic representation of a volume profile for the reaction A + B → AB in which three possible locations for the transition state are indicated (see text).

which represents the volume changes due to electrostriction and other effects acting on the surrounding solvent molecules during the activation process and the overall reaction [1]. It is principally the intrinsic volume of activation $\Delta V^{\neq}_{int}$ that is considered as the mechanistic indicator in the case of substitution and related reactions. The mechanistic assignment for processes in which no major solvational changes occur is, in fact, straightforward, since bond formation should result in a negative $\Delta V^{\neq}_{int}$ value and bond breakage in a positive one. In recent years a number of groups have been involved in theoretical calculations in efforts to account for the experimentally observed volume data. References to these studies are included in this presentation and reviewed elsewhere [5].

For high pressure kinetic studies in coordination chemistry the pressure range is usually limited to 300 MPa. Such pressures can significantly effect the value of a rate or equilibrium constant, which forms the basis of all treatments of activation and reaction volume data. It is important to note that very high pressures are not needed since activation and reaction volumes are determined from the pressure dependence of rate and equilibrium constants extrapolated to ambient pressure. Various instruments for the study of slow and fast reactions, including flow systems and relaxation techniques, have been developed. A detailed discussion on these is presented in two recent reviews [14,15]. The techniques involve stopped flow, T-jump, P-jump, NMR, ESR, pulsed-laser and pulse-radiolysis instrumentation. They cover a kinetic time range from hours and days to nano- and picoseconds. In general the pressure dependence of rate and equilibrium constants can be determined to a high degree of accuracy, and the experimental error limits on reaction and activation volume data are usually only a few $cm^3\ mol^{-1}$.

The impressive progress made in the development of fast reaction techniques and the handling of oxygen sensitive samples at elevated pressure has stimulated the progress made in inorganic, organometallic and bioinorganic mechanistic studies. Volumes of activation exhibit some important advantages over entropies of activation: they can be determined more accurately; their interpretation is less difficult; their magnitude can be visualized or estimated with the help of models; and their values can be correlated with partial molar volumes of reactant and product species in the ground state to construct a reaction volume profile.

The interpretation of the pressure dependence of a rate constant is based on a simplified version of the transition state theory, which does not take the dynamics of the reactant–solvent interaction into account [1–4]. This simplification usually applies to non-diffusion-controlled processes and has been adopted in the examples presented in this account.

3. Ligand substitution reactions

Ligand substitution reactions of coordination compounds have been the topic of many mechanistic investigations because of the fundamental importance of such reactions in chemical and biological processes. For a ligand substitution reaction in general, there are basically three simple pathways: (i) the dissociative (D) process,

with an intermediate of lower coordination number, (ii) the associative (A) process, with an intermediate of higher coordination number, and (iii) the interchange (I) process, in which no intermediate of lower or higher coordination number is involved, and in which either bond breakage (I_d) or bond formation (I_a) is the more important process. Such bond formation/bond breakage processes should be characterized by specific intrinsic volume changes.

For symmetrical solvent or ligand exchange reactions, the volume of activation will be a direct measure of the degree of bond formation/bond breakage in the transition state, keeping in mind that some extension or compression of the non-participating ligand bond lengths occur during such processes. A continuous spectrum of transition states can be envisaged, ranging from a very expanded, highly dissociative one (large positive $\Delta V^{\neq}$), to a very compact, highly associative one (large negative $\Delta V^{\neq}$). The overall reaction volume ΔV for such symmetrical reactions is zero. The experimental data reported for such processes [1,2,4–8] clearly demonstrate the sensitivity of $\Delta V^{\neq}$ towards the size of the metal center and coordinated ligands (i.e. solvent molecules) which in fact tunes the intimate nature of the exchange process in terms of the preference for bond formation or bond breakage processes. (Further details are presented in another contribution in this issue).

Non-symmetrical ligand substitution reactions are classified along the same lines as symmetrical solvent ligand exchange reactions and exhibit pressure dependencies that correlate closely with those found for solvent exchange processes [1,2,4,5]. The substitution can be of one ligand for another where neither is the solvent (ligand for ligand substitution), it can be substitution where one (or more) ligands attached to a metal center is (are) replaced by one or more solvent molecules (e.g. aquation, solvolysis, base hydrolysis), or it can be a reaction of a solvated metal ion in which one or more coordinated solvent molecules are replaced by one or more ligands (complex-formation or anation). Thus the products and the reactants are different, unlike the case for solvent exchange reactions. In terms of volume changes these reactions are of considerable interest, since the partial molar volumes of reactants and products will, in general, differ. Thus, the volume profile will consist of volumes of activation in both directions, as well as the overall reaction volume. The latter may be obtained directly or indirectly depending on the kinetic accessibility and other properties of the system. The partial molar volume of the product(s) can be greater than both the partial molar volumes of the reactants and transition state, or smaller than both or intermediate between that of the reactants and transition state (see Fig. 1). In favorable examples, the volume profile can be developed on an absolute scale rather than only on a relative volume basis, when direct measurements of partial molar volumes of reactants and products (via density measurements) can be made.

3.1. Thermal ligand substitution reactions

In the case of a nonsymmetrical ligand substitution reaction, the volume profile reveals the location of the transition state with respect to the reactant and product

states, such that $\Delta V^{\neq}$ can be related to the reaction volume ΔV. The formation of the mono bipyridine complexes of Zn(II) and Cd(II) aqua ions [16,17] provides excellent straightforward examples of both size influence on mechanistic determination and complements activation volume and reaction volume measurements. An improved access to the coordinated solvent by the ligand in the outer sphere permits an I_a mechanism for formation of $Cd(bpy)(H_2O)_4^{2+}$, a process not possible in the formation of the analogous Zn(II) complex, which is formed from a smaller hexaaqua ion, resulting in an I_d mechanism. Fig. 2 displays the volume profiles for these two complex-formation reactions. The mechanism proposed for the zinc complex-formation is entirely consistent with recent calculations for water exchange on $Zn(H_2O)_n^{2+}$ [18]. Density functional theory has been applied successfully to describe the water exchange mechanism for aquated Zn(II), Pd(II) and Pt(II) cations [18,19]. The optimized transition state structure for the Zn(II) ion clearly demonstrates the dissociative nature of the process; in no way could a seventh water molecule be forced to enter the coordination sphere without the simultaneous dissociation of one of the six coordinated water molecules.

Aquation and solvolysis reactions of octahedral and square-planar complexes, i.e. the reverse reaction of the complex-formation discussed above, also exhibit very characteristic $\Delta V^{\neq}$ values. One of the most exciting examples involves the aquation of pentaammine complexes of Co(III) and Cr(III), for which controversial arguments have been reported in the literature. A study of a series of aquation reactions involving neutral leaving ligands, in order to reduce possible contributions resulting from changes in electrostriction, revealed $\Delta V^{\neq}$ values in good agreement with those found for the water-exchange processes. The data support the operation of an I_a mechanism in the case of Cr(III) complexes compared to an I_d mechanism in the case of Co(III) complexes [20,21].

Typical dissociatively activated substitution reactions of pentacyanoferrate(II) and (III) complexes exhibit quite large and positive $\Delta V^{\neq}$ values [11,22–29]. Solvolysis of the pentacyanonitroferrate(III) ion has been studied in several solvents, and the rate constants for displacement of nitrite correlated with the electron donor ability of the solvent. It was concluded, based on the values of $\Delta V^{\neq}$ and other considerations, that the solvent interacts with the cyanide ligands and an increase in the electron density on the metal center contributes to inducing a dissociative mechanism.

A volume profile has been constructed for the aquation and the reverse complex-formation reaction in the case of amminepentacyanoferrate(II) (Fig. 3) [29]. The very similar volumes of activation found for both the forward and reverse reactions result from the rather similar partial molar volumes of NH_3 (24.8 cm^3 mol^{-1}) and H_2O (18.0 cm^3 mol^{-1}) and the apparent insensitivity of $\Delta V^{\neq}$ for a limiting D mechanism toward the size of the leaving group [5].

The values of $\Delta V^{\neq}$ for substitution of a range of substituted pyridine ligands and other leaving group variants from pentacyanoferrate(II) complex ions by CN^- in aqueous solution are all positive and vary little, consistent with a D mechanism. There are reasonable correlations between the logarithm of the rate constants and the pK_a values and also the values of $\Delta V^{\neq}$ for uncharged leaving groups from this and other studies [25].

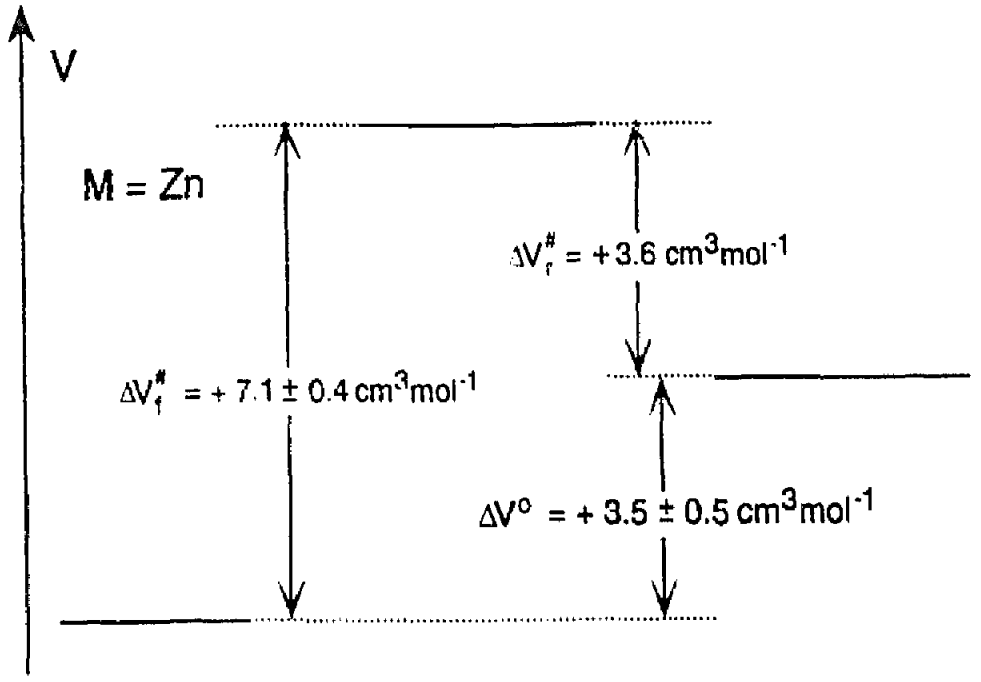

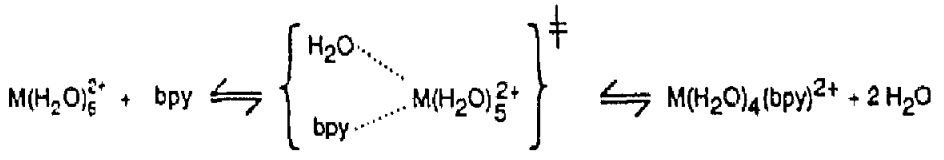

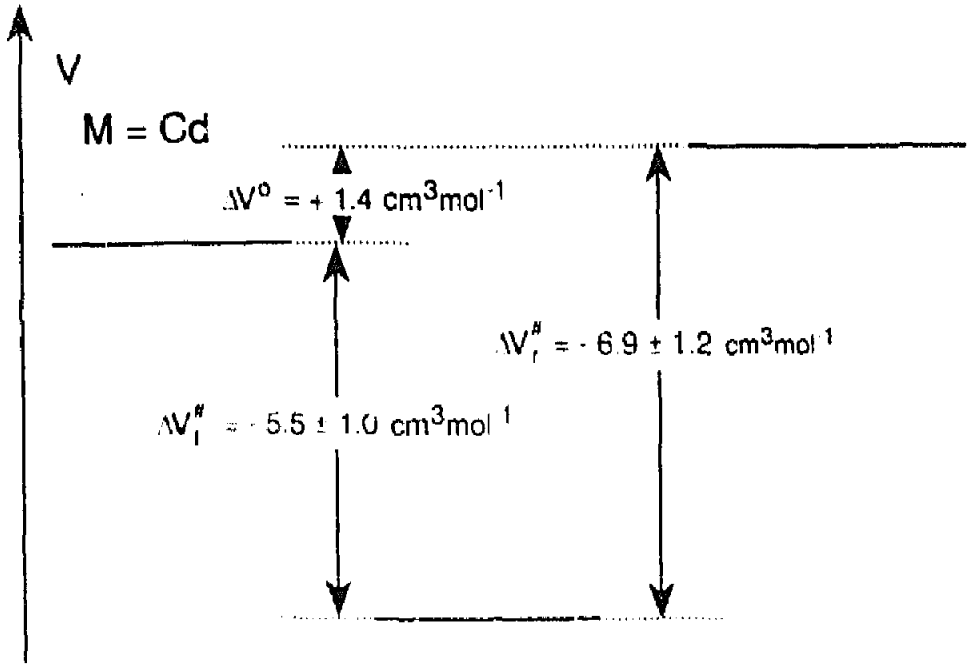

Fig. 2. Volume profiles for formation and dissociation of $M(H_2O)_4(bpy)^{2+}$ complexes; M = Zn, Cd [16,17].

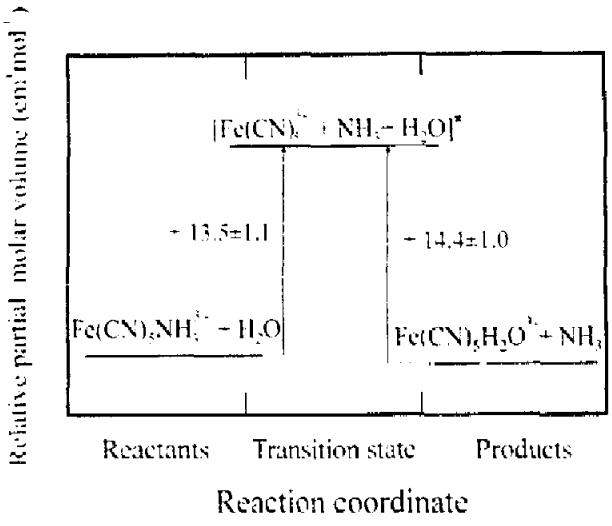

Fig. 3. Volume profile for the overall reaction [29]: $Fe(CN)_5NH_3^{2-} + H_2O \leftrightarrow Fe(CN)_5H_2O^{2-} + NH_3$.

Another type of ligand substitution reaction that exhibits an interesting and remarkable pressure dependence is base-catalyzed aquation (base hydrolysis reaction). The kinetics and mechanism of base hydrolysis of Co(III) pentaammine complexes have fascinated chemists for decades, and have been compared with and contrasted to those of corresponding reactions of Cr(III) complexes. At present, the $\Delta V^{\neq}$ data available for more then 30 different Co(III) complexes vary, depending on the charge on the leaving ligand, between $+19$ and $+43$ cm^3 mol^{-1} [30,31]. The distinctly positive values can be explained by charge neutralization and release of a solvent molecule in the pre-equilibrium conjugate base formation step, followed by ligand dissociation in the rate limiting step. Although a wide selection of the non-hydrolyzing ligands was employed, the results indicated a relative insensitivity to their nature. Volume profiles were developed for these processes. Overall, the results clearly demonstrate the intrinsic and solvational volume changes that occur within the proposed S_N1CB mechanism for these reactions.

Base hydrolysis of chromium(III) pentaammine complexes in which the departing ligand is Cl^-, is also characterized by large positive $\Delta V^{\neq}$ values [32]. The reaction volume for the pre-equilibrium conjugate base formation step could be estimated to be 22 cm^3 mol^{-1}, giving rise to $\Delta V^{\neq}$ values for the rate determining ligand substitution step ranging from -5 to $+13$ cm^3 mol^{-1}, signifying a mechanistic changeover from I_d to I_d or D throughout the series for substitution on the conjugate base species. The outcome of the competition between the Cr–Cl bond breakage and the addition of solvent is controlled by the nature of the non-substituting ligands to the extent that when the latter cause steric hindrance, a more dissociative mechanism is promoted. The results [33] for base hydrolysis of some halopentaammine and related complexes of Cr(III), in some of which the non-hydrolyzing ligands are aliphatic amines, also indicate that an associative interchange is occurring, underlining the difference from similar reactions for Co(III) complexes.

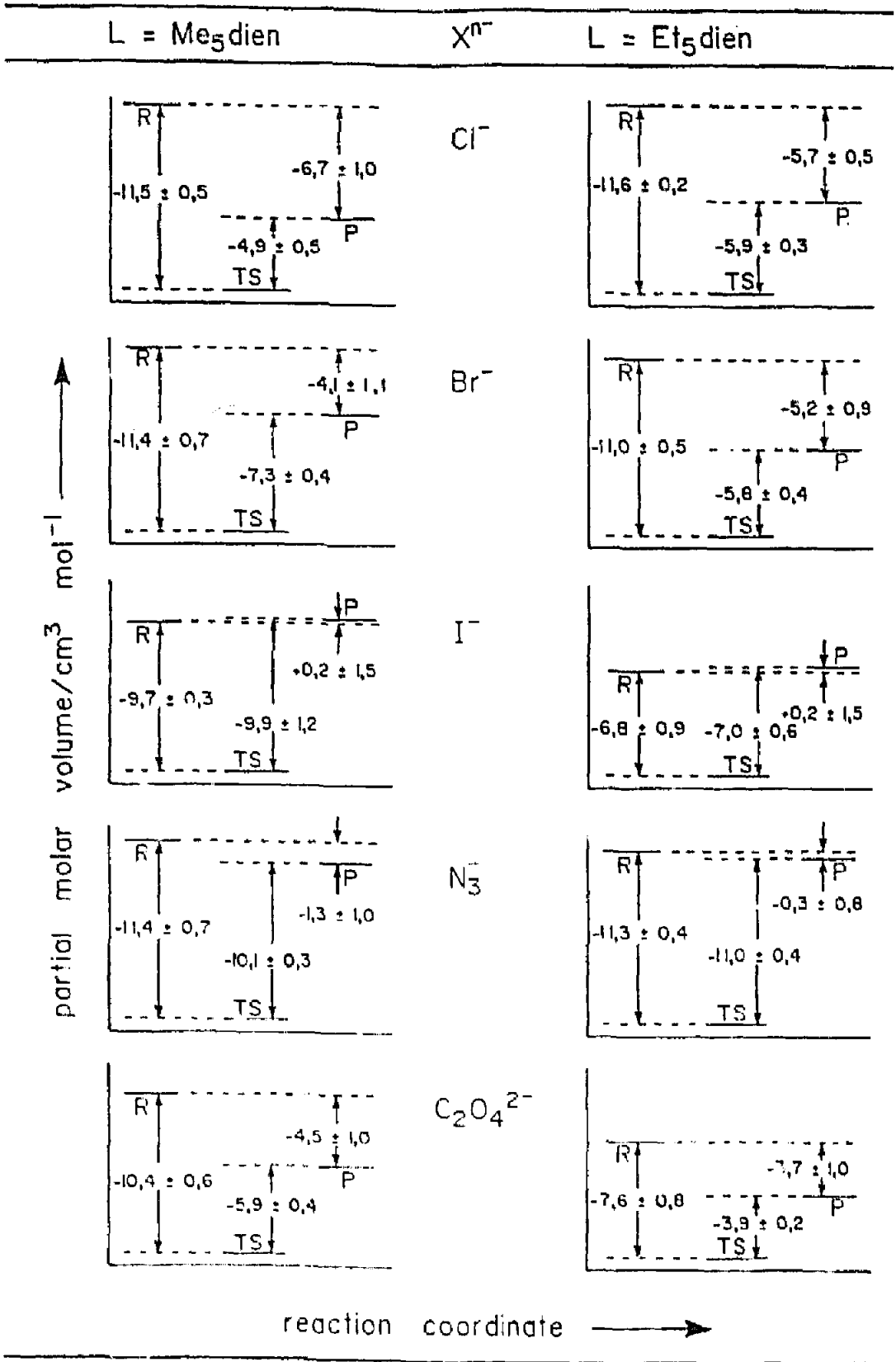

R = reactants; TS = transition state; P = products

Fig. 4. Volume profiles for the reaction [38]: $Pd(L)X^{(2-n)+} + H_2O \Leftrightarrow Pd(L)H_2O^{2+} + X^{n-}$.

Solvolysis reactions of diethylentriamine (dien) and substituted dien complexes of Pd(II) exhibit large and negative $\Delta V^{\neq}$ values in agreement with an associative mechanism [34]. Introduction of steric hindrance (Me or Et substituents on the dien ligand) decreases the solvolysis rate constants by up to six orders of magnitude, but does not affect the nature of the substitution mechanism since both $\Delta S^{\neq}$ and $\Delta V^{\neq}$ remain large and negative. The nature of the leaving group does affect the value of $\Delta V^{\neq}$ and may indicate the operation of an I_d mechanism [35]. Nevertheless, the observation that the steric hindrance alone cannot change the nature of the substitution mechanism for square planar complexes is very significant [36,37]. With the available $\Delta V^{\neq}$ for both complex-formation and reverse aquation reactions of Pd(II) complexes, it is possible to construct reaction volume profiles for the overall processes. A few examples are given in Fig. 4, from which it follows that the transition state has a significantly lower partial molar volume than either the reactant or product species, demonstrating the associative character of the substitution process even when taking possible electrostriction effects into account [38].

Solvolysis of the Pd(II) complexes of pentamethylated dien and one pyridine ligand by six different solvents proceeds in each case by an associative process with no immediately obvious correlation between $\Delta V^{\neq}$ and any property of the solvents [39]. The aquation and the reverse process of anation of *rac*-$Pt(R_5\text{-en})Cl_2$ occur in two steps each possessing transition states of smaller volume than either reactant or product, as illustrated in Fig. 5, with the consequence of an I_d mechanism for both steps in the forward direction [40,41].

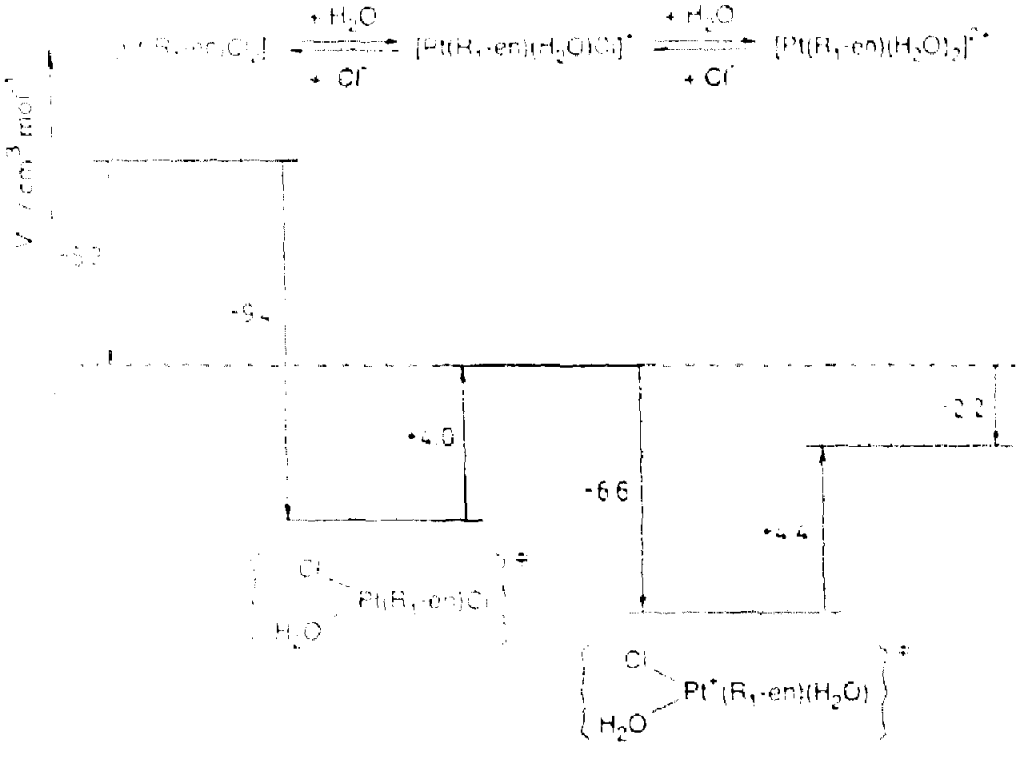

Fig. 5. Volume profile for two steps reversible aquation of [Pt(R$_5$-en)Cl$_2$]. First step at 311.3 K, and second at 275.0 K [41].

There are a number of important biological and medical processes in which ligand substitution reactions on transition metal centers play an important role. One of these concerns the antitumor activity of platinum complexes, for which it is generally accepted that substitution reactions involving the metal complexes and DNA moieties play a key role in such processes [42]. In general these substitution reactions follow an associative mechanism and are therefore usually characterized by markedly negative volumes of activation, i.e. the reactions are accelerated by pressure. For example, binding of ligands such as inosine and inosine monophosphate to Pd(II) centers in which three coordination sites are non-substituting occurs by an associative mode of activation [43]. When the non-substituting ligands on Pd(II) ions are ethylenediamine (en) and Et_4en, each of the observed kinetic processes depends on the nucleoside concentration [44]. The binding and dissociation (aquation) of the nucleosides occur associatively.

A further example concerns the substitution reactions of cobalamins (vitamin B_{12}), which have attracted considerable attention from kineticists. In these systems the usually kinetically inert Co(III) ion is labilized considerably by the corrin ring, and there has been some disagreement in the literature concerning the mechanism of these substitution reactions. The volume of activation data available for complex-formation and reverse aquation reactions of the type:

$$B_{12}\text{–}H_2O^{+} + L^{n} \rightleftharpoons B_{12}\text{–}L^{(1-n)+} + H_2O \qquad (1)$$

are all in support of a dissociative (I_d) substitution mechanism [45–50]. For the reaction of B_{12}–H_2O^{+} with pyridine, the observed rate constants reached a limiting value at high ligand concentrations. This is due to a precursor-formation step preceding the dissociative interchange step. The nonlinear concentration dependence enabled a kinetic separation of the precursor-formation constant and the rate-determining interchange rate constant to be made, such that a detailed volume profile for the overall process could be drawn (see Fig. 6). The volume profile clearly illustrates the dissociative character of the transition state.

Recently, evidence was reported for the unexpected associative displacement of adenosyl by cyanide in coenzyme B_{12} [51]. This evidence included, in addition to other kinetic observations, a $\Delta V^{\neq}$ value of -10.0 ± 0.4 cm^3 mol^{-1}. Various possible reaction mechanisms were suggested to account for the associative nature of the process.

3.2. *Labilization effects in thermal substitution reactions*

In recent years an interest in tuning the substitution lability of metal complexes via a systematic variation of the steric and electronic properties of the coordinated spectator ligands has developed. Such variations can cause a drastic change in lability of the exchangable ligand and the fundamental question is whether or not this is accompanied by a gradual changeover in the mechanism of the substitution reaction.

The mechanistic understanding of solvent exchange reactions has reached the point where specific labilization effects can be studied in a systematic way. In this

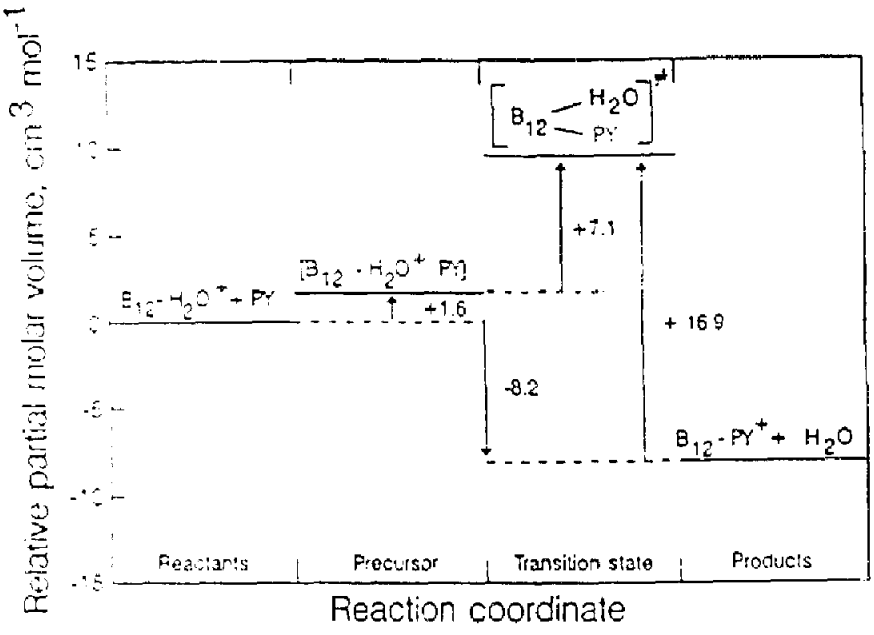

Fig. 6. Volume profile for the reaction [47,49]: $B_{12}\text{-}H_2O^{+} + py \Leftrightarrow B_{12}\text{-}py^{+} + H_2O$.

respect it is appropriate to refer to significant *trans*-labilization caused by the deprotonation of a coordinated water molecule. In the case of hexaaqua complexes of Fe(III), Rh(III) and Ir(III), such deprotonation can cause an increase in the water exchange rate of between 700 and 20 000 times at 298 K [52]. This labilization is also accompanied by a changeover in mechanism from a more associative interchange mechanism for hexaaqua complex ions to a more dissociative interchange mechanism for the pentaaquamonohydroxo complex ions. As a result of rapid proton exchange, labilization by coordinated hydroxide is not site specific, with the result that all five coordinated water molecules are labilized to the same extent. Recent studies [53] on the effect of pressure on the water exchange reaction of the dihydroxo bridged Rh(III) dimer demonstrated that coordinated water molecules located *cis* and *trans* to the hydroxo bridging ligands exhibit different chemical shifts, and exchange significantly faster with the bulk solvent than with the bridging hydroxo groups. Surprisingly, these water molecules exchange at a rather similar rate (ca. 10^2 faster than water exchange on the hexaaquarhodium(III) monomer, but ca. 10^2 slower than exchange on the pentaaquamonohydroxo monomer). The estimated volumes of activation were found to be between +9 and +10 cm^3 mol^{-1}, which is a clear indication for a dissociative exchange mechanism. The surprising similarity in the exchange rates of the *cis* and *trans* water molecules becomes quite understandable in terms of a limiting dissociative mechanism [53].

Phosphite ligands such as $P(OEt)_3$ are known to labilize the *trans* position. Detailed kinetic studies were performed on complex-formation and the reverse aquation reactions for complexes of the type *trans*-$[Ru(NH_3)_4\{P(OEt)_3\}(H_2O)]^{2+}$ for a range of organic and inorganic entering ligands in aqueous solution [54]. Based on the volume of activation data and the constructed volume profiles (see Fig. 7), a dissociative interchange mechanism was proposed, e.g. the data suggested

that bond breaking is more important than bond making in the transition state, independent of the nature of the entering ligand, viz. nucleophile or electrophile.

Other examples of large labilization effects include the introduction of metal–carbon bonds on traditionally inert metal centers such as Co(III), Rh(III), and Ir(III). For instance, the presence of Cp* in the complexes $M(Cp^*)(H_2O)_3^{2+}$ (M = Rh(III) and Ir(III)) causes an increase in the solvent exchange rate constant of 10^{14} as compared to the hexaaqua species [55]. The volumes of activation support the operation of a dissociative interchange mechanism in both cases. In the case of the $Co(NH_3)_5CH_3^{2+}$ complex, the strong *trans* labilization caused by the metal–carbon bond does not only show up in the ground state structure [56], but also causes this complex to become extremely labile. The substitution reaction is characterized by a large and positive volume of activation, suggesting a limiting dissociative mechanism [57]. The introduction of carbon bonded alkyls on rhodoximes also causes a drastic increase in the lability of the *trans* position. The nature of the organic ligand not only controls the rate of the substitution process, but also the nature of the mechanism. Based on the reported volumes of activation [58], it could be concluded that CH_3 induces a fast substitution process that follows a dissociative interchange mechanism, whereas for the weaker CH_2CF_3 donor group, the substitution reaction is significantly slower and follows an associative interchange mechanism. A typical volume profile constructed for the reversible binding of iodide in the case of the methyl complex is shown in Fig. 8. Interestingly enough, whether the organic group was varied or not for a given nucleophile, all

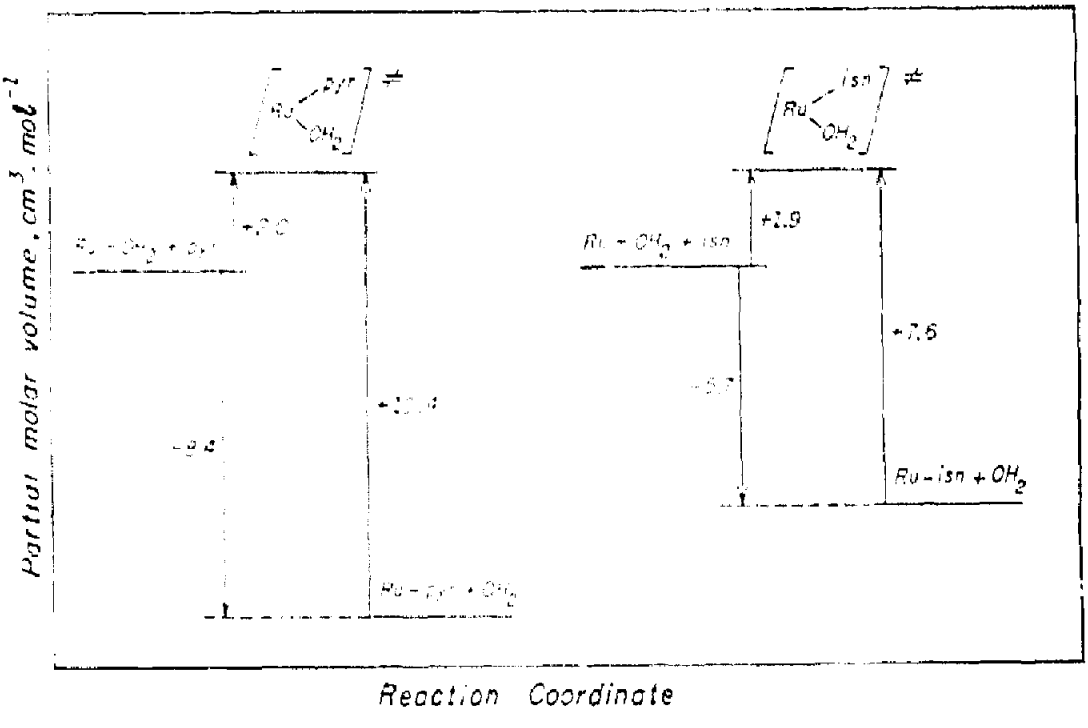

Fig. 7. Volume profiles for the reaction [54] *trans*-$[Ru(NH_3)_4(P(OEt)_3)(H_2O)]^{2+}$ + L ⇌ *trans*-$[Ru(NH_3)_4(P(OEt)_3)L]^{2+}$ + H_2O, where L = pyrazine (left) or isonicotinamide (right). The metal complexes are shown in abbreviated forms.

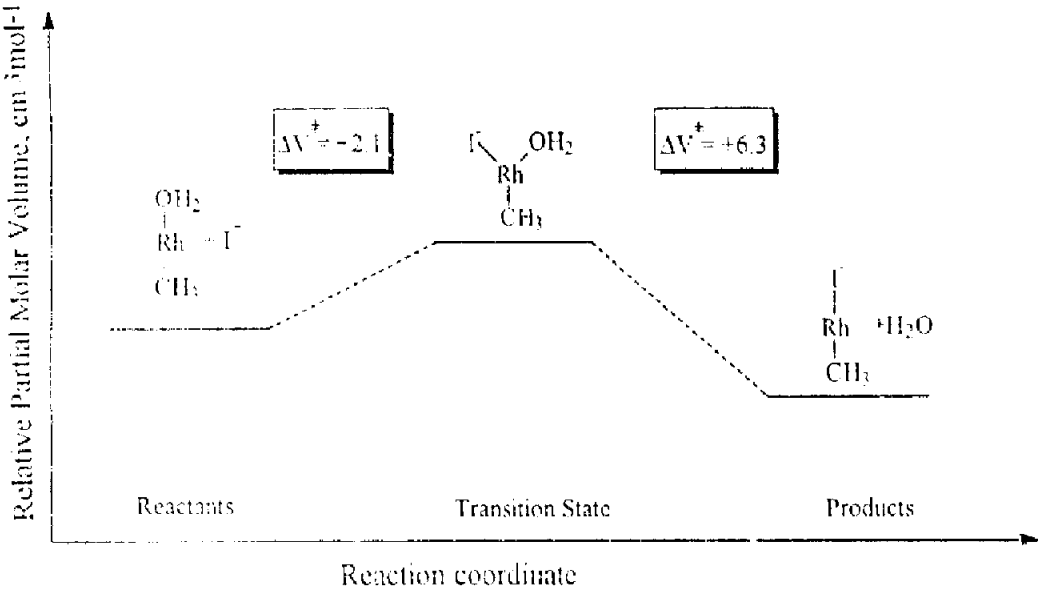

Fig. 8. Volume profile for the nucleophilic substitution of *trans*-Rh(III)(dmg)$_2$(CH$_3$)(H$_2$O) by iodide [58].

reactions studied were characterized by moderately negative entropies of activation, which by contrast demonstrates the mechanistic discrimination power of pressure versus temperature as a physical variable.

The introduction of metal–carbon bonds in square-planar complexes has also resulted in significant labilization effects. The basic question dealt with, was the possibility to find evidence for a changeover in the substitution mechanism of such systems. In general d^8 systems follow an associative substitution mechanism, but specific labilization effects may induce a dissociative substitution mode. The introduction of a single metal–carbon bond in benzylamine complexes of the type Pt(C,N,N)H$_2$O$^+$ and Pt(N–C–N)H$_2$O$^+$ [59,60], caused an increase in lability of the coordinated water molecule by a factor of 10^4 in comparison to a complex of the type Pt(N,N,N)H$_2$O^{2+}. However, the activation volumes clearly indicated that the substitution reactions still follow an associative mechanism. A typical volume profile for one of the systems is reported in Fig. 9. The increase in lability in these complexes was accounted for in terms of an increase in the electrophilicity of the metal center due to back bonding effects with the in plane benzyl chelate. It is clear from a comparison with other literature data [37,61] that more than one metal–carbon bond is required in order to cause a changeover to a dissociative substitution mode. There are a number of papers dealing with substitution reactions of Pt(II) complexes containing two metal–carbon σ-bonds in the *cis*-arrangement. As σ-donors C$_6$H$_5$, 4-MeC$_6$H$_4$, C$_6$F$_5$ and CH$_3$ were used, and dmso and different thioethers were the labile leaving groups [62–64]. For all systems parallel associative and dissociative reaction paths were observed. Evidence for the occurrence of the unusual dissociative reaction mode in such systems was obtained from positive $\Delta V^{\neq}$ values reported for the investigated reactions [64].

Solvent exchange and ligand substitution reactions can be drastically affected by the influence of chelating ligands. For instance, solvent exchange on $Fe(H_2O)_6^{3+}$ occurs at a rate of 2×10^2 s^{-1} at 298 K and is characterized by an activation volume of -5.4 cm^3 mol^{-1}, typical for an associative interchange mechanism [65]. Introduction of hexadentate chelating ligands such as ethylendiaminetetraacetate, cyclohexyldiaminetetraacetate and phenylenediaminetetraacetate to produce seven-coordinate complexes of the type $Fe^{III}(L)H_2O^{-}$, results in solvent exchange rates of ca. 10^7 s^{-1} at 298 K (i.e. an acceleration of 10^5) and volumes of activation of between $+3.2$ and $+4.6$ cm^3 mol^{-1}, which are typical for a dissociative interchange process [66,67]. Thus the increase in lability is once again accompanied by a changeover in the nature of the ligand substitution mechanism. In the case of substitution reactions on Ru(III), the lability of the hexaaqua complex can be increased by up to six orders of magnitude by introducing a chelating ligand such as ethylendiaminetetraacetate (edta) into the coordination sphere [68,69]. A series of ligands have been chosen for displacing the water in both $Ru(edta)(H_2O)^{-}$ and $Ru(hedta)(H_2O)$. The markedly rapid substitution in the former case was suggested to be due to distortion of metal–ligand bonds and labilization of the coordinated water molecule arising from H-bonding between the free carboxylate and the coordinated water. Both sets of reactions proceed by an associatively activated substitution process based on the interpretation of the activation volumes data [68–70].

Introduction of a multidentate ligand into the coordination sphere of an aquated metal ion can also cause a change in coordination geometry accompanied by a drastic decrease in lability. One such example involved ligand substitution reactions on Cu(II). The extremely rapid dissociative solvent exchange on $Cu(H_2O)_6^{2+}$ [71] is slowed down by three orders of magnitude for the trigonal bipyramidal $Cu(tren)H_2O^{2+}$ ion, where tren = 2,2′,2″-triaminotriethylamine. The complex-formation reaction of the five coordinate $Cu(tren)H_2O^{2+}$ with neutral nucleophiles involves no change in charge, so the reported activation and reaction volumes are mainly due to intrinsic volume changes associated with the ligand substitution

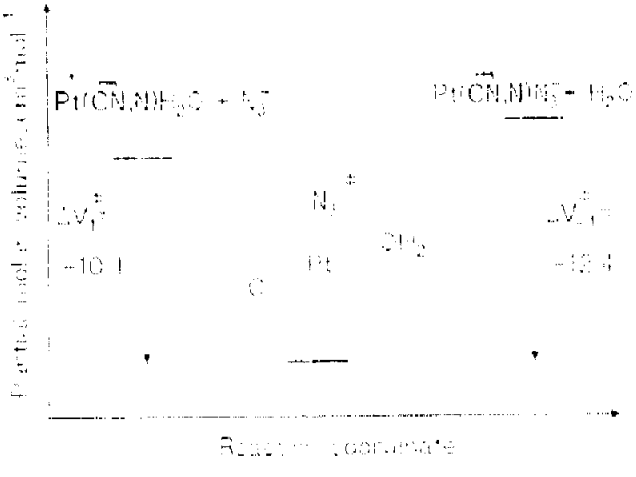

Fig. 9. Volume profile for anation of $PtCl(CN_4NH_3O)$ by azide [59].

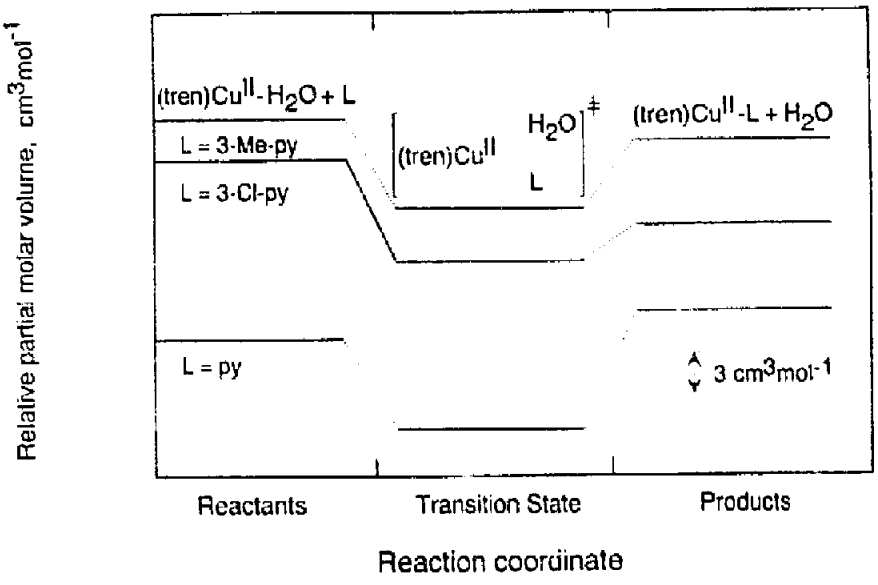

Fig. 10. Volume profiles for complex formation reactions of Cu(tren)H_2O^{2+} by a series of pyridine ligands [72].

process [72]. Typical values for $\Delta V^{\neq}$ are between -7 and -10 cm^3 mol^{-1} for the displacement of water by the entering nucleophile, and between -5 and -9 cm^3 mol^{-1} for the reverse aquation reactions. The volume profile in Fig. 10 clearly demonstrates the compact nature of the transition state compared to that of either the reactant or product states. By way of comparison, $\Delta V^{\neq}$ for solvent exchange on Cu(tren)H_2O^{2+} has a value of -4.7 ± 0.2 cm^3 mol^{-1}, which clearly demonstrates the common mechanism in operation during solvent exchange and ligand substitution reactions. In terms of the ligand substitution mechanism, this volume collapse is characteristic for an associative interchange (I_a) mechanism. In general, octahedral Cu(II) complexes undergo a very fast dissociative interchange (I_d) ligand substitution mechanism characterized by a positive volume of activation [71]. The significant changeover in mechanism observed for the Cu(tren)H_2O^{2+} complex [72] is related to its unique trigonal bipyramidal structure, which eliminates the Jahn–Teller distortion and results in a significantly slower associative substitution reaction. Such results clearly demonstrate the ability of volume profile analyses to discriminate between thermal ligand substitution mechanisms. Further modification of the tren ligand to Me_3tren and Me_6tren drastically affects the coordination geometry as well as the lability of the complexes [73,74]. Ligand substitution reactions of Cu(Me_3tren)H_2O^{2+} are characterized by less negative volumes of activation than in the case of Cu(tren)H_2O^{2+}, but these are still in line with an I_a substitution mechanism.

3.3. Photochemical and photoinduced ligand substitution

Ligand photosubstitution reactions are the most widely studied photoreactions of metal complexes. The first quantitative studies of pressure effects on such reactions

were performed for a series of $Cr(NH_3)_5X^{(3-n)+}$ complexes [75], for which it was postulated that exchange of X^{n-} or NH_3 occur via different excited states. The pressure dependence of these reactions resulted in significantly negative apparent $\Delta V^{\neq}$ values for both aquation of NH_3 and aquation of X^{n-}. Since little was known about the pressure dependence of the other deactivation processes, it was assumed that these apparent values represent those for the primary photoreactions. Accordingly, the data were interpreted in terms of an associative (most probably I_a) substitution process. The more negative values found for the aquation of X^{n-} as compared to NH_3 were ascribed to solvational contributions originating from charge creation (i.e. electrostriction) in the transition state. A more recent detailed reanalysis of the data [76] also supported the mechanistic conclusions in terms of an associative nature of the substitution process.

Significantly more progress has been made in the study of photosolvolysis reactions of Rh(III) ammine complexes [77,78]. For complexes of the type $Rh(NH_3)_5X^{(3-n)+}$, the photosubstitution of X^{n-} or NH_3 for solvent molecules can occur. It was generally found that the two photolysis reactions exhibit opposite pressure effects. Similarly, the pressure dependence of the excited-state lifetime, measured by pulsed laser techniques, also exhibited different trends depending on the major photochemical reaction observed. Throughout the series of complexes, solvolysis of NH_3 is accompanied by a positive $\Delta V^{\neq}$ value, whereas the solvolysis of X^{n-} exhibits negative values. Both these values can be interpreted in a qualitative way in terms of a dissociative mechanism. The substantial difference in $\Delta V^{\neq}(k_p)$ for the halide and ammine labilizations can be ascribed to a negative contribution from $\Delta V^{\neq}_{cr}$ due to charge creation when the halide dissociates from the dipositive complex to form a tripositive cation and X^{n-}. No appreciable charge creation is expected for the dissociation of NH_3. This difference also shows up in the overall ΔV for the ground-state ligand substitution process of +3.9 and −17.8 $cm^3\ mol^{-1}$, respectively, in the case of the $Rh(NH_3)_5Cl^{2+}$ complex [77], demonstrating the important contribution of charge creation when the leaving group is anionic.

In systems like those discussed above, the interpretation of the data is sometimes complicated by solvational contributions that play a role when net charge creation or neutralization is involved during the substitution process. Therefore, in more recent studies the pressure dependence of some typical organometallic photosubstitution reactions including low valence metal centers and neutral ligands were investigated. A series of photosubstitution reactions of the type:

$$M(CO)_6 + L \xrightarrow{h\nu} M(CO)_5L + CO \qquad (2)$$

(M = Cr, Mo, W; L = σ donor ligand)

were studied as a function of pressure for various L and solvents [79]. For all reactions investigated the photosubstitution quantum yield decreased with increasing pressure and resulted in significantly positive volumes of activation. Under the assumption that nonradiative deactivation is relatively independent of pressure, the apparent positive volumes of activation fit well into the picture of a dissociative

mechanism, i.e. release of CO. This dissociation leads to a trigonal bipyramidal $M(CO)_5$ fragment that can either recombine with CO, be trapped by a solvent molecule or bind to L. The difference in the pressure dependence for the recombination with CO or combination with L can be used to account for the observed activation volumes.

Numerous data [80–82] are now available for the photosubstitution reactions of the type:

$$M(CO)_4(phen) + L \xrightarrow{h\nu} fac\text{-}M(CO)_3(phen)L + CO \quad (3)$$

(M = Cr, Mo, W; L = PMe_3, PEt_3)

There has been some controversy in the literature concerning the nature of the photo-substitution mechanism originating from the lower lying MLCT state. On the one hand it was assumed that the observed photo-substitution proceeds dissociatively from the LF excited state, i.e. MLCT excitation is followed by thermal back population of the LF state. On the other hand it was argued that the MLCT states themselves are photoactive and could in principle undergo an associative substitution reaction. In order to resolve this apparent discrepancy, the effect of pressure on the above reaction as a function of irradiation wavelength, i.e. LF and MLCT excitation, was studied [80–84]. The first results for L = PEt_3 clearly suggested an associative substitution mechanism for the Mo and W complexes when irradiated directly into the MLCT bands. This was indicated by negative $\Delta V^{\neq}$ values for 546 nm irradiation, in contrast to positive $\Delta V^{\neq}$ values for ligand substitution when LF bands were excited with 366 nm light. In the case of the smaller Cr complex, MLCT excitation still gave a small positive value of $\Delta V^{\neq}$ indicative of a dissociative mechanism. The associative character of the MLCT states could be accounted for in terms of partial transfer of electron density from the metal to the phen ligand, by which the metal became more electrophilic and could undergo nucleophilic attack by the entering ligand. More recently, in a series of studies [82–84] there was a systematic investigation of the influence of the metal center, entering nucleophile, and irradiation wavelength as a function of pressure for various M (M = Cr, Mo, W) and PR_3 (R = Me, Bu^n, Ph). The competition between dissociative LF and associative MLCT ligand substitution could be tuned by selecting the appropriate metal, entering ligand, ligand concentration and pressure. The typical results displayed in Fig. 11 show how an increase in irradiation wavelength from LF to MLCT excitation results in a changeover in the effect of pressure on φ, viz. a decrease in φ with increasing pressure for irradiation at 313 and 366 nm, compared to an increase in φ with increasing pressure for irradiation at 436–546 nm. The results showed that the size of the metal center and the entering nucleophile determine the irradiation wavelength at which a mechanistic changeover occurs. The bulkier the entering nucleophile, the more difficult it is to observe an associative mechanism resulting from MLCT excitation.

A number of other types of photochemical reactions involving organometallic systems have recently been studied as a function of pressure in efforts to gain more insight into the details of the underlying reaction mechanisms. These include carbonylation and metal–metal bond homolysis reactions [85,86].

Flash photolysis techniques have in general been adopted with success to study thermal substitution and electron-transfer processes of reactive intermediates. In these systems one deals with pressure effects on subsequent thermal reactions that occur with unstable species generated in solution photochemically that have relevance for instance in catalytic and biological processes. The interpretation of $\Delta V^{\neq}$ data and volume profiles is more straightforward than in the case of the photochemical processes itself, since we are dealing with reaction rate constants determined directly and the associated pressure dependence of these, without the added complications of competing photophysical decays. For example, flash photolysis has been adopted to study the substitution behavior of reactive intermediates in organometallic chemistry. Irradiation of $M(CO)_6$ (M = Cr, Mo, W) in a coordinating solvent (S) produces intermediates of the type $M(CO)_5S$ [87,88], which can undergo rapid solvent displacement by a nucleophile (L) to produce $M(CO)_5L$ as shown in Eq. (4).

$$M(CO)_6 + S + h\nu \rightarrow M(CO)_5S + L, \quad \text{fast} \tag{4}$$

$$M(CO)_5S + L \rightarrow M(CO)_5L + S, \quad \text{slow}$$

The effect of pressure on such substitution reactions has been studied for a series of M, S, and L. The results (Table 1) demonstrate the roles played by the size of the metal center (M), the bulkiness of the ligand (L), and the coordination ability of the solvent (S). The data exhibit a trend to more negative (less positive) $\Delta V^{\neq}$ values for larger metal centers [87,88].

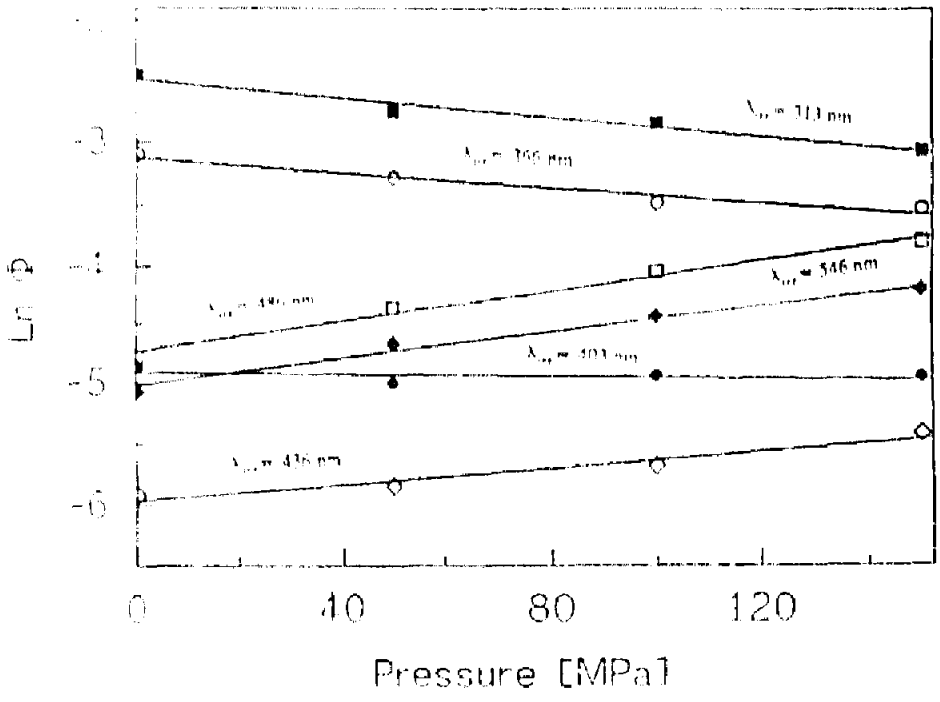

Fig. 11. Plot of natural logarithm of the quantum yield versus pressure at different excitation wavelengths for the reaction [84]: $M(CO)_4(phen) + PR_3 \rightarrow fac\text{-}M(CO)_3(PR_3)(phen) + CO$; (M = Mo, R = Bu^n)

Table 1
Summary of $\Delta V^{\neq}$ data for solvent displacement reactions of the type: $M(CO)_5S + L \rightarrow M(CO)_5L + S$

S	L	$\Delta V^{\neq}$ ($cm^3 mol^{-1}$)		
		M = Cr	M = Mo	M = W
Fluorobenzene	1-Hexene	$+9.4 \pm 0.7$	$+5.8 \pm 0.8$	$+2.5 \pm 0.2$
Toluene		$+10.8 \pm 0.7$	$+3.2 \pm 0.3$	
Benzene		$+10.9 \pm 1.0$		
Chlorobenzene		$+5.4 \pm 0.4$	$+3.2 \pm 0.3$	$+0.4 \pm 0.3$
n-Heptane		$+6.2 \pm 0.2$	$+2.2 \pm 0.3$	$+2.7 \pm 0.4$
Fluorobenzene	Piperidine	$+6.1 \pm 0.3$		
Toluene		$+4.8 \pm 1.4$		
Benzene		$+4.2 \pm 0.3$		
Chlorobenzene		$+0.2 \pm 0.2$		
n-Heptane		$+1.4 \pm 0.4$		

When the attacking nucleophile is a bidentate ligand, flash photolysis of $M(CO)_6$ results in the reaction sequence outlined in Eq. (5), in which ring closure involves CO displacement:

$$M(CO)_6 + h\nu \rightarrow M(CO)_5 + CO \tag{5}$$

$$M(CO)_5 + S \rightarrow M(CO)_5S, \quad \text{fast}$$

$$M(CO)_5S + N{-}N \rightarrow M(CO)_5N{-}N + S, \quad k_1$$

$$M(CO)_5N{-}N \rightarrow M(CO)_4(N{-}N) + CO, \quad k_2$$

Table 2
Summary of $\Delta V^{\neq}$ data for the ring-closure step in Eq. (5)

M	Solvent	N N[a]	k_2 at 25°C s^{-1}	$\Delta H^{\neq}$ ($kJ\ mol^{-1}$)	$\Delta S^{\neq}$ ($J\ K^{-1} mol^{-1}$)	$\Delta V^{\neq}$ ($cm^3\ mol^{-1}$)
Cr	Toluene	en	1.6×10^{-3}	57 ± 5	-145 ± 17	-11.9 ± 1.5
	Toluene	$dabR_2$	1.5×10^{-4}	81 ± 2	-47 ± 7	$+17.2 \pm 1.0$
	Fluorobenzene	phen	26	52 ± 2	-42 ± 6	$+6.2 \pm 0.5$
Mo	Toluene	en	3.0×10^{-2}	72 ± 7	-92 ± 22	-5.4 ± 0.8
	Toluene	$dabR_2$	1.1×10^{-3}	78 ± 5	-40 ± 17	-9.5 ± 0.4
	Fluorobenzene	phen	$1.1 \times 10^{+1}$	47 ± 2	-9 ± 7	-2.9 ± 0.2
W	Toluene	en	3.0×10^{-4}	54 ± 2	-172 ± 16	-12.3 ± 1.4
	Toluene	$dabR_2$	2.9×10^{-3}	83 ± 8	-53 ± 26	-13.7 ± 1.3
	Toluene	bpy	8.0×10^{-2}	58 ± 2	-74 ± 7	-10.9 ± 1.1
	Fluorobenzene	phen	4.3×10^{-1}	51 ± 2	-23 ± 5	-8.2 ± 0.2

[a] Abbreviations: en, ethylenediamine; $dabR_2$, 1,4-diisopropyl-1,4-diazabutadiene; bpy, bipyridine; phen, 1,10-phenanthroline.

Table 3
Activation volumes for chelate ring closure in $M(CO)_5L$ complexes in toluene (M = Mo, W)

L[a]	M	$\Delta V^{\neq}$ ($cm^3\ mol^{-1}$)
bpy	Mo	-3.9 ± 0.6
	W	-10.9 ± 1.1
dmbpy	Mo	-5.6 ± 0.4
	W	-8.4 ± 1.0
dpbpy	Mo	5.4 ± 0.5
	W	-6.4 ± 0.6
dbubpy	Mo	6.2 ± 1.0
	W	-4.5 ± 0.2

[a] Abbreviations: bpy, 2,2'-bipyridine; dmbpy, 4,4'-dimethyl-2,2'-bipyridine; dpbpy, 4,4'-diphenyl-2,2'-bipyridine; dbubpy, 4,4'-di-*tert*-butyl-2,2'-bipyridine.

Typical data for a series of ring-closure reactions are summarized in Table 2, from which it follows that the nature of the metal center and the bulkiness of N–N control the intimate nature of the CO displacement mechanism [89]. The larger metal centers (Mo, W) tend to exhibit significantly negative $\Delta V^{\neq}$ values suggesting ring closure in an associative reaction mode. The smaller Cr center must lose CO prior to ring closure since only in the absence of steric hindrance on the entering ligand, as in the case of ethylenediamine, does an associative ring-closure occur.

More recently, systematic studies of the effect of bulky substituents on bpy and phen ligands, as well as the influence of the solvent on ring-closure reactions of $M(CO)_5N$–N (M = Mo and W) were undertaken [90,91]. The results for a series of bipyridine ligands (see Table 3) clearly indicate a change in $\Delta V^{\neq}$ from small negative to small positive values on increasing the steric hindrance on the Mo complex. This observation can be ascribed to a gradual change in mechanism from I_a to I_d on increasing steric hindrance of the ligand. A similar trend is observed for the W complexes, although the overall $\Delta V^{\neq}$ value remains negative throughout the series of ligands. In this case, the values suggest that ring closure remains associative, although a gradual change from limiting associative (A) to an interchange associative (I_a) mechanism may occur on increasing the steric hindrance. Throughout the series of complexes the $\Delta V^{\neq}$ values are more negative for W than for Mo, which indicates that the W metal center has a greater ability to undergo bond formation with the ring-opened chelate.

Activation volumes have also been measured for the above reactions in supercritical fluids and found to be as large as $+7$ l mol^{-1} under conditions near the critical point in supercritical ethane and CO_2 [90,92]. The results were interpreted as evidence for a large repulsive contribution to the activation volume associated with the dissociation of CO during the ring-closure reaction.

3.4. Radiation-induced ligand substitution

The mechanism of inorganic and organometallic free radical reactions, such as the formation of metal–carbon σ bonds, can conveniently be studied by using pulse-radiolysis techniques. Such processes are closely related to substitution reactions, although they usually involve a formal change in the oxidation state of the metal center due to the covalent nature of the metal–carbon σ bond.

Application of high pressure pulse-radiolysis techniques has made possible the construction of volume profiles for the formation and dissociation of metal–carbon σ bonds. In the first such study, it could be shown that the formation of a cobalt–carbon bond is assisted by pressure in the reaction of $Co^{II}(nta)(H_2O)_2^-$ with $^{\bullet}CH_3$ to produce $Co^{III}(nta)(H_2O)(CH_3)^-$ [93]. This is due to an overall reaction volume of -16.4 ± 1.6 cm^3 mol^{-1} (determined from the pressure dependence of the equilibrium constant) which results from a small positive volume of activation for the forward bond formation process and a large positive volume of activation for the reverse homolysis reaction. The volume profile in Fig. 12 clearly indicates the higher partial molar volume of the transition state and underlines the operation of a dissociative mechanism for the entrance of the radical into the coordination sphere of the Co(II) complex. In fact, the small positive $\Delta V^{\neq}$ for the cobalt–carbon bond formation reaction suggests that the process follows an I_d mechanism and is presumably controlled by solvent exchange on $Co(nta)(H_2O)_2^-$. The significantly larger volume of activation for the reverse homolysis reaction is partly ascribed to desolvation of the aliphatic free radicals formed during the reaction.

Similar results were reported [94] for the formation of complexes of the type $Cr(H_2O)_5R^{2+}$ in which $^{\bullet}R$ is an aliphatic radical that forms a metal–carbon σ

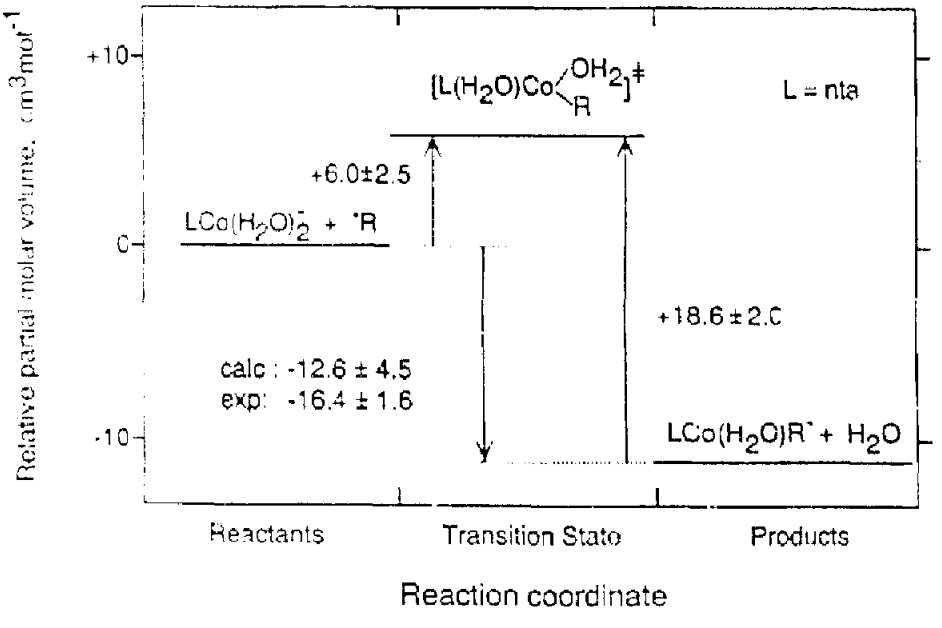

Fig. 12. Volume profile for the reaction of methyl radicals with the nitrilotriacetate complex of Co(II) at 298 K [93].

bond with Cr^{2+}. This reaction was studied for ten different radicals, and the reactions all exhibit a small positive volume of activation with an average value of $+4.3 \pm 1.0$ cm^3 mol^{-1}, independent of the nature of R. This constant value and the fact that the bond formation rate constants are all very similar and close to that for the water exchange process on $Cr(H_2O)_6^{2+}$, suggests that the complex-formation reaction is controlled by an I_d ligand exchange mechanism. The dissociative nature of the ligand exchange process is presumably enhanced by Jahn–Teller distortion in $Cr(H_2O)_6^{2+}$, similar to that reported for $Cu(H_2O)_6^{2+}$ [95].

Pulse radiolysis studies of the oxidation of Cu(II) complexes by $^{\bullet}OH$ radicals have shown that transient Cu(III) complexes are formed. The effect of pressure on the formation of the various Cu(III) complexes has been studied in order to assist the elucidation of the underlying reaction mechanism. The reaction between $^{\bullet}OH$ radicals and $[Cu^{II}(P_2O_7)_2(H_2O)_2]^{6-}$ resulted in the formation of a Cu(III) complex [96]. No reaction is observed with $N_3^{\bullet}$ or $Br_2^{\bullet}$ whereas $SO_4^{-\bullet}$ initiates the same steps as seen with $^{\bullet}OH$. This suggests that the mechanism probably involves a ligand interchange or $H^{\bullet}$ atom abstraction process. The Cu(III) complex undergoes a rapid first-order reaction, probably loss of the $P_2O_7^{4-}$ chelate, followed by addition of OH^- to yield a Cu(III) complex that is predominantly hydroxylated and has a relatively long half life. Strong support for this mechanism comes from the very small activation volume found for the first step. The value of -1.8 ± 0.7 cm^3 mol^{-1} is in close agreement with that found for the reactions of Cu^{2+}(aq) with $^{\bullet}OH$ radicals [97]. Furthermore, it was recently reported that electron-transfer reactions between metal ions and radicals that are not diffusion controlled, exhibit pressure dependencies that support a ligand-substitution controlled process [98]. The slightly negative volume of activation found for the reaction of $[Cu^{II}(P_2O_7)_2(H_2O)_2]^{6-}$ with $^{\bullet}OH$ can therefore be interpreted as evidence for a pure interchange (I) or an associative interchange (I_a) mechanism that controls the interaction between these two species.

4. Electron-transfer reactions

Significant progress has been made in the application of high pressure thermodynamic and kinetic techniques to the study of inorganic and bioinorganic electron-transfer reactions during the last 10 years. Especially in the case of self-exchange reactions, which represent the simplest symmetrical electron-transfer process, it has been possible to account for the observed pressure effects in terms of the Marcus-Hush theory. In the case of nonsymmetrical electron-transfer reactions, the volume changes are primarily due to solvent reorganization from changes in electrostriction associated with the electron-transfer process.

Symmetrical self-exchange reactions are the simplest kind of electron-transfer process, since there is no net chemical reaction and no reaction volume, and therefore in principle the mechanistic interpretation of activation volume data, as in the case of solvent exchange reactions, is relatively straightforward. One of the first interesting observations was that the activation volume for self-exchange on

$Fe(H_2O)_6^{3+/2+}$ is ca. 12 $cm^3\ mol^{-1}$ more negative than that for self-exchange on $Fe(H_2O)_5OH^{2+/+}$ $Fe(H_2O)_6^{2+}$ [99]. The difference could be explained in terms of the operation of an outer-sphere mechanism in the former process and an inner-sphere mechanism in the latter case, since the formation of a hydroxo bridged species will be accompanied by the release of a solvent molecule, i.e. a markedly more positive activation volume.

Another interesting example involves the self-exchange reaction between MnO_4^{-} and MnO_4^{2-} for which $\Delta V^{\neq}$ has a value of -21 $cm^3\ mol^{-1}$ [100]. This reaction is catalyzed by counter ions such as Na^+ and K^+ and the catalysis manifests itself in very different $\Delta V^{\neq}$ values. The same group [101] has studied an extensive series of self-exchange reactions and found a good correlation between experimental and theoretically calculated values. In general, solvent reorganization accounts for the largest contribution towards the observed activation volume, which has in many cases a negative value. In some cases, viz. $Co(en)_3^{3+/2+}$ and $Co(phen)_3^{3+/2+}$ the theoretical volume of activation was found to be significantly larger than the experimental value, which was ascribed to the participation of high-spin to low-spin changeover associated with the electron-transfer process. More recently, the group demonstrated that volumes of activation for homogeneous self-exchange reactions can be obtained from volumes of activation for heterogeneous self-exchange reactions on the surface of an electrode [102]. A detailed account on electrode reactions of metal complexes in solution at high pressures is included in this issue [103].

4.1. Non-symmetrical electron-transfer reactions

One objective of many mechanistic studies dealing with inorganic electron-transfer reactions has been to distinguish between outer-sphere and inner-sphere mechanisms. High pressure kinetic methods and analysis of reaction volume profiles have been employed to provide a better understanding of the intimate mechanism involved in such processes. The differentiation between outer-sphere and inner-sphere mechanisms depends on the nature of the precursor species, Ox/Red in the following scheme, which can either be an ion pair or encounter complex, or a bridged intermediate, respectively.

$$Ox + Red \Leftrightarrow Ox\ \ Red, \quad K \tag{6}$$

$$Ox\ \ Red \rightarrow Ox'\ \ Red', \quad k_{11}$$

$$Ox'\ \ Red' \Leftrightarrow Ox' + Red'$$

This means that the coordination sphere of the reactants remains intact in the former case and is modified by ligand substitution in the latter, which will naturally affect the associated volume changes.

A difficulty encountered in many cases in kinetic studies of outer-sphere electron-transfer processes concerns the separate determination of the precursor formation constant (K) and the electron transfer rate constant (k_{11}) (in the scheme outlined above), from an empirically determined composite parameter. In the majority of

cases, precursor formation is a diffusion controlled step, followed by rate-determining electron transfer. In the presence of an excess of Red, the rate expression is given by:

$$k_{obs} = k_{ET}K[Red]/(1 + K[Red]) \quad (7)$$

In many cases K is small, such that this equation simplifies to $k_{obs} = k_{ET}K[Red]$, which means that the observed second-order rate constant and the associated activation parameters are composite quantities, viz. $\Delta V^{\neq} = \Delta V^{\neq}(k_{ET}) + \Delta V(K)$. When K is large enough such that $1 + K[Red] > 1$, it is possible to separate k_{ET} and K kinetically and also the associated activation parameters, viz. $\Delta V^{\neq}(k_{ET})$ and $\Delta V(K)$.

A series of reactions were studied where it was possible to resolve K and k_{ET}, and thereby $\Delta V(K)$ and $\Delta V^{\neq}(k_{ET})$. In this case, oppositely charged reaction partners were selected as indicated in the following general scheme:

$$Co(NH_3)_5X^{(3-n)+} + Fe(CN)_6^{4-} \Leftrightarrow [Co(NH_3)_5X^{(3-n)+} \cdot Fe(CN)_6^{4-}], \quad K \quad (8)$$

$$[Co(NH_3)_5X^{(3-n)+} \cdot Fe(CN)_6^{4-}] \rightarrow Co^{2+} + 5NH_3 + X^{n-} + Fe(CN)_6^{3-}, \quad k_{ET}$$

$$X^{n-} = H_2O, Me_2SO, py, Cl^-, N_3^-$$

The data [104] indicated that ion pair formation is accompanied by close to zero ΔV values. This is rather surprising, since it is generally accepted that ion-pair formation should involve considerable charge neutralization accompanied by strong desolvation due to a decrease in electrostriction. Values of ΔV therefore indicate that the reaction partners most probably exist as solvent-separated ion-pairs, i.e. with no significant charge neutralization accompanied by desolvation. It is evident that the electron transfer steps exhibit a strong pressure deceleration, with most systems having $\Delta V^{\neq}$ values of between +25 and +34 $cm^3\ mol^{-1}$. These values indicate that electron transfer is accompanied by extensive desolvation, most probably related to charge neutralization associated with the electron-transfer process. A simplified model based on partial molar volume data, in which electron transfer occurs within the precursor ion-pair $[Co(NH_3)_5X^{(3-n)+} \cdot Fe(CN)_6^{4-}]$, leading to the successor ion-pair $[Co(NH_3)_5X^{(2-n)+} \cdot Fe(CN)_6^{3-}]$, predicts an overall volume increase of ca. 65 $cm^3\ mol^{-1}$. This means that according to the $\Delta V^{\neq}$ values mentioned above, the transition state for the electron-transfer process lies approximately halfway between the reactant and product states on a volume basis for the precursor and successor ion-pairs. The largest volume contribution arises from the oxidation of $Fe(CN)_6^{4-}$ to $Fe(CN)_6^{3-}$, which is accompanied by a large decrease in electrostriction and an increase in partial molar volume of ca. 40 $cm^3\ mol^{-1}$ [1,105]. Theoretical calculations also confirmed that the transition state for these reactions lies approximately halfway along the reaction coordinate on a volume basis [106]. This first information on the nature of the volume profile for an outer-sphere electron-transfer reaction proved to be in good agreement with the results reported subsequently for systems with a low driving force in which it was possible to construct a complete volume profile by studying the effect of pressure on both the forward and the reverse reactions, as well as on the overall equilibrium constant.

More recently outer-sphere redox reactions between $[Co(N)_5H_2O]^{3+}$ / $[Co(N)_5OH]^{2+}$ ($(N)_5$ = tetraazacycloamine ligands) and $Fe(CN)_6^{4-}$ have been studied as a function of $(N)_5$, temperature and pressure in order to establish possible correlations between, on the one hand, the size, geometry and charge of the cobalt(III) complex and on the other hand, the outer-sphere formation constant, the electron transfer rate constant, and thermal and pressure activation parameters [107]. The values obtained indicate that outer-sphere formation constants are, within the experimental error, the same for all the systems studied. The electron transfer rate constants for the $[Co(N)_5H_2O]^{3+}$ complexes increase on increasing the size of the macrocyclic ligand independently of its *cis* or *trans* geometry. For the $[Co(N)_5OH]^{2+}$ complexes, the same trend is observed but the differences are smaller. The thermal and pressure activation parameters are those expected for these types of reactions and are interpreted in view of combined effects of electrostatic and hydrogen bonding interactions. All the $\Delta V^{\neq}$ values are very positive and arise from changes in electrostriction associated with charge neutralization (especially $Fe(CN)_6^{4-}$ to $Fe(CN)_6^{3-}$) and a volume increase on reduction of Co(III) to Co(II). For all the systems studied, the value of $\Delta V^{\neq}$ obtained for the hydroxo complex is consistently lower than that of its aqua counterpart. The lower activation volume values found for the hydroxo systems have to be related to the absence of contributions arising from the reduction of Co(III) to Co(II), both due to charge differences (absence of a 3+ cation) and bond distances (shorter Co–O bond), that is the increased compactness of the L cage.

Recent conventional and high pressure investigations on the intermolecular electron-transfer reaction between myoglobin and hexacyanoferrate(III) have shown that both oxy- and deoxymyoglobin are redox active species [108]. The rate and activation parameters underline the operation of an outer-sphere mechanism for both systems. Precursor formation is accompanied by significant desolvation, especially around the $[Fe(CN)_6]^{3-}$ moiety. The strongly negative $\Delta V^{\neq}(k)$ value found for the reaction with oxymyoglobin partially results from a large volume decrease due to the reduction of $[Fe(CN)_6]^{3-}$ to $[Fe(CN)_6]^{4-}$ accompanied by some volume increase due to the release of dioxygen.

Data are also available for the reduction of $Fe(CN)_5L^{n-}$ (where $L = CN^-$, NO_2^-), $Ru(CN)_6^{3-}$ and aquated Fe(III), by ascorbic acid and ascorbate ions [106,109–111]. The penta-, and hexacyano complexes all exhibit a strongly negative volume of activation that results mainly from the increase in electrostriction due to the reduction of $M(CN)_5L^{n-}$ (M = Fe, Ru). In the case of aquated Fe(III) species, the activation volumes are significantly positive: these have been ascribed to an outer-sphere electron-transfer reaction in the case of $Fe(H_2O)_6^{3+}$, but to an inner-sphere reaction in the case of the more labile $Fe(H_2O)_5OH^{2+}$ complex [106].

The interpretation of volume changes associated with electron-transfer reactions has benefited considerably from work on high pressure electrochemistry performed by Tregloan and coworkers [105,112]. They systematically investigated the effect of pressure on the redox potentials of a series of transition metal complexes, and from the associated reaction volumes for the redox couples could distinguish between intrinsic and solvational volume contributions in such reactions.

There is much interest in the oxidation of polyaminocarboxylate complexes of Fe(II) by molecular oxygen and hydrogen peroxide mainly due to the fundamental importance of such reactions in biochemical processes, such as the cleavage of DNA, the decomposition of H_2O_2, and the dismutation of superoxide. All oxidation reactions of chelated Fe(II) complexes studied as yet, are found to be accelerated by pressure and accompanied by significantly negative volumes of activation [113]. These can be ascribed to the bonding of dioxygen that is accompanied by the oxidation of Fe(II) to Fe(III) and the reduction of dioxygen to superoxide and peroxide ions, processes that are all expected to lead to a decrease in partial molar volume. In a recent reinvestigation of the Fe^{II}(edta) oxidation reaction it was possible to resolve the different reaction steps that form part of the oxidation process, and to assign the negative volumes of activation in a more detailed way [114,115].

4.2. Long-distance electron-transfer reactions

A challenging question concerns the feasibility of the application of high pressure kinetic and thermodynamic techniques in the study of long-distance electron-transfer reactions. Do such processes exhibit a characteristic pressure dependence, and to what extent can a volume profile analysis reveal information on the intimate mechanism of the electron-transfer process?

The systems investigated were intermolecular and intramolecular electron-transfer reactions between ruthenium complexes and cytochrome *c* [116–119]. A series of intermolecular reactions between chelated cobalt complexes and cytochrome *c* were also studied [120]. A variety of high pressure experimental techniques, including stopped-flow, flash-photolysis, pulse-radiolysis and voltammetry, were employed in these investigations. A remarkably good agreement was found between the volume data obtained with the aid of these different techniques, which clearly demonstrates that these different methods for the study of electron-transfer processes compliment each other.

Application of pulse-radiolysis techniques revealed that the following intramolecular and intermolecular electron-transfer reactions all exhibit a significant acceleration with increasing pressure. The reported volumes of activation are -17.7 ± 0.9, -18.3 ± 0.7, and -15.6 ± 0.6 cm^3 mol^{-1}, respectively, for the three reactions, and denote a marked volume reduction as the reaction proceeds from the reactant to the transition state [119].

$$(NH_3)_5Ru^{II}\text{-(His33)cyt } c^{III} \rightarrow (NH_3)_5Ru^{III}\text{-(His33)cyt } c^{II} \quad (9)$$

$$(NH_3)_5Ru^{II}\text{-(His39)cyt } c^{III} \rightarrow (NH_3)_5Ru^{III}\text{-(His39)cyt } c^{II}$$

$$Ru^{II}(NH_3)_6^{2+} + \text{cyt } c^{III} \rightarrow Ru^{III}(NH_3)_6^{3+} + \text{cyt } c^{II}$$

At this stage it was uncertain what the negative volumes of activation really meant since overall reaction volumes were not available. However data in the literature [121] suggested that the oxidation of $Ru(NH_3)_6^{2+}$ to $Ru(NH_3)_6^{3+}$ is accompanied by a volume decrease of ca. 30 cm^3 mol^{-1}, which would mean that

the activation volumes quoted above could mainly arise from volume changes associated with the oxidation of the ruthenium redox partner.

In order to obtain further information on the magnitude of the overall reaction volume and the location of the transition state along the reaction coordinate, a series of intermolecular electron-transfer reactions of cytochrome *c* with pentaammineruthenium complexes were studied, where the sixth ligand on the ruthenium complex was selected in such a way that the overall driving force was low enough so that the reaction kinetics could be studied in both directions [117,118]. The selected substituents were isonicotinamide (isn), 4-ethylpyridine (4-etpy), pyridine (py), and 3,5-lutidine (lut). The overall reaction can be formulated as:

$$Ru^{III}(NH_3)_5L^{3+} + \text{cyt } c^{II} \Leftrightarrow Ru^{II}(NH_3)_5L^{2+} + \text{cyt } c^{III}, \quad k_f, k_b \tag{10}$$

For all the systems investigated, the forward reaction was significantly decelerated by pressure, whereas the back reaction was significantly accelerated by pressure. The absolute values of the volumes of activation for the forward and reverse processes were indeed very similar, demonstrating that a similar rearrangement occurred in order to reach the transition state. In addition, the overall reaction volume for these systems could be determined spectrophotometrically by recording the spectrum of an equilibrium mixture as a function of pressure, and electrochemically by recording cyclic and differential pulse voltammograms as a function of pressure [122]. These results are summarized along with kinetic data and activation parameters in Table 4. A comparison of the ΔV data demonstrates the generally good agreement between the values obtained from the difference in the volumes of activation for the forward and reverse reactions, and those obtained thermodynamically. Furthermore, the values also clearly demonstrate that $\Delta V^{\neq} = 0.5|\Delta V|$, i.e. the transition state lies approximately halfway between the reactant and product states on a volume basis, independent of the direction of electron transfer. The typical volume profile in Fig. 13 presents the overall picture, from which the location of the transition state can clearly be seen.

Similar results were recently obtained for the redox reactions of a series of cobalt imine complexes with cytochrome *c* [120,123]. In general a good agreement exists between the kinetically and thermodynamically determined parameters, and the typical volume profile in Fig. 14 once again demonstrates the symmetrical location of the transition state with respect to the reactant and product states. Since it is known that oxidation of cytochrome *c* is accompanied by small volume changes [122], the observed volume changes were ascribed to volume changes on the redox partner and not on cytochrome *c* itself. This was suggested by the fact that the change in partial molar volume associated with the oxidation of the investigated Ru(II) and Co(II) complexes as obtained from electrochemical and density measurements, almost fully accounted for the observed overall reaction volume. Thus the reduction of cytochrome *c* can only make a minor contribution towards the overall volume change.

The results obtained for the above systems demonstrate that the resulting picture is very consistent and allows a further detailed analysis of the data. The overall reaction volumes determined in four different ways are surprisingly similar and

Table 4
Summary of rate and activation parameters for the electron-transfer reaction between cytochrome *c* and several pentaammineruthenium complexes [117]: $Ru^{II}H_2O(NH_3)_5L^{2+} + cyt\ c(II) \leftrightarrows Ru^{III}H_2O(NH_3)_5L^{3+} + cyt\ c(III)$

Reaction	k_r ($M^{-1}\ s^{-1}$)[a]	$\Delta H^{\neq}$ (kJ mol^{-1})	$\Delta S^{\neq}$ (J $K^{-1}\ mol^{-1}$)	$\Delta V^{\neq}$ ($cm^3\ mol^{-1}$)	ΔV° ($cm^3\ mol^{-1}$)	$-\Delta G^{\circ}$ (eV)	K_f[b]	K_{UV}[b]	K_{KIS}[b]
$Ru^{II}H_2O(a)$-lutidine + cyt *c*(II)	27 144 ± 1271	35.4 ± 0.3	−41 ± 1	+16.9 ± 1.4	33.6 ± 1.7[c]	0.012	1.6	2.6 ± 0.1	2.9 ± 0.4
$Ru^{III}H_2O(a)$-lutidine + cyt *c*(III)	9448 ± 516	21 ± 1	−99 ± 5	17.8 ± 1.6	34.7 ± 1.6[c]				
$Ru^{II}H_2O(a)$-etpy + cyt *c*(II)	26 823 ± 477	29 ± 2	−61 ± 7	+14.7 ± 0.9	26.9 ± 1.8[c]	0.011	1.5	2.2 ± 0.4	2.9 ± 0.1
$Ru^{III}H_2O(a)$-etpy + cyt *c*(III)	9182 ± 124	25 ± 2	−86 ± 6	14.9 ± 1.1	29.6 ± 1.0[d]				
$Ru^{II}H_2O(a)$-py + cyt *c*(II)	48 620 ± 1161	28 ± 1	−64 ± 5	+17.4 ± 1.5	33.4 ± 1.9[c]	0.045	5.8	6.4 ± 2.1	4.6 ± 0.4
$Ru^{III}H_2O(a)$-py + cyt *c*(III)	10 517 ± 494	33 ± 4	−59 ± 13	17.7 ± 0.8	35.1 ± 1.0[d]				
$Ru^{II}H_2O(a)$-isn + cyt *c*(II)	1.15×10^5	22 ± 1	−75 ± 3	+16.0 ± 0.9	31 ± 1[c] 26.4 ± 0.9[e]	0.112	78	71 ± 7	75.7
$Ru^{III}H_2O(a)$-isn + cyt *c*(III)	1520 ± 130	28 ± 4	−87 ± 12	17.2 ± 1.5	33.2 ± 1.3[d]				

[a] Reaction conditions: T 25°C; μ 0.1 M; [cyt *c*] 1×10^{-5} M; [Tris] 0.05 M; [$LiClO_4$] 0.05 M; pH 7.1; λ = 550 nm.
[b] Equilibrium constant for the oxidation of cytochrome *c*.
[c] Reaction volume determined spectrophotometrically for the oxidation of cytochrome *c*.
[d] Reaction volume determined kinetically for the oxidation of cytochrome *c*.
[e] Ref. [122].

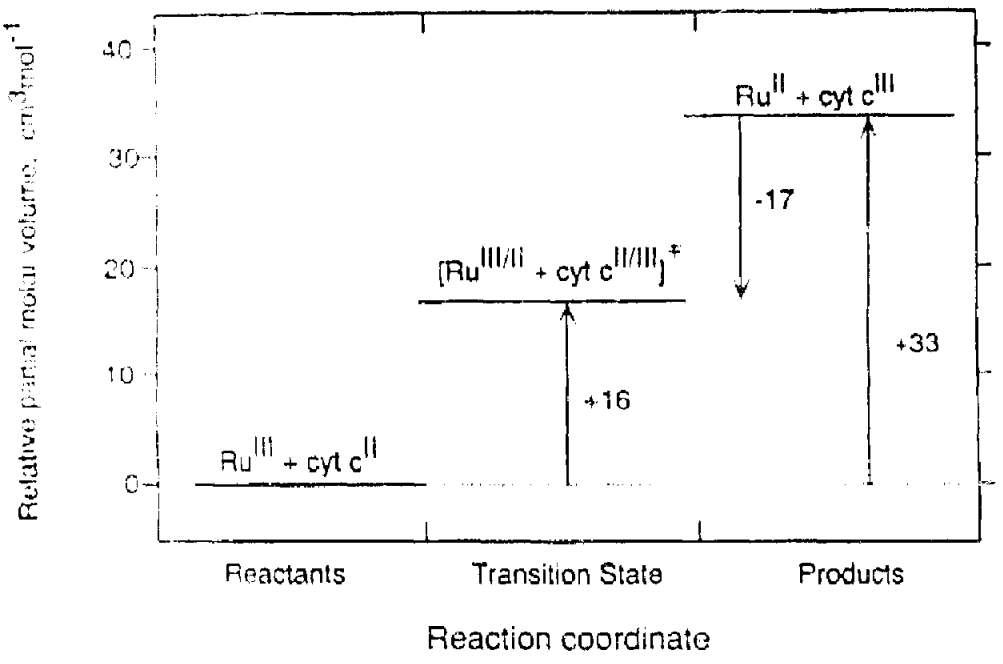

Fig. 13. Volume profile for the reaction of an isonicotinamide pentaammine ruthenium complex with cytochrome c at 298 K [117].

underline the validity of the different methods employed. The volume profiles in Figs. 13 and 14 demonstrate the symmetric nature of the intrinsic and solvational reorganization in order to reach the transition state of the electron-transfer process.

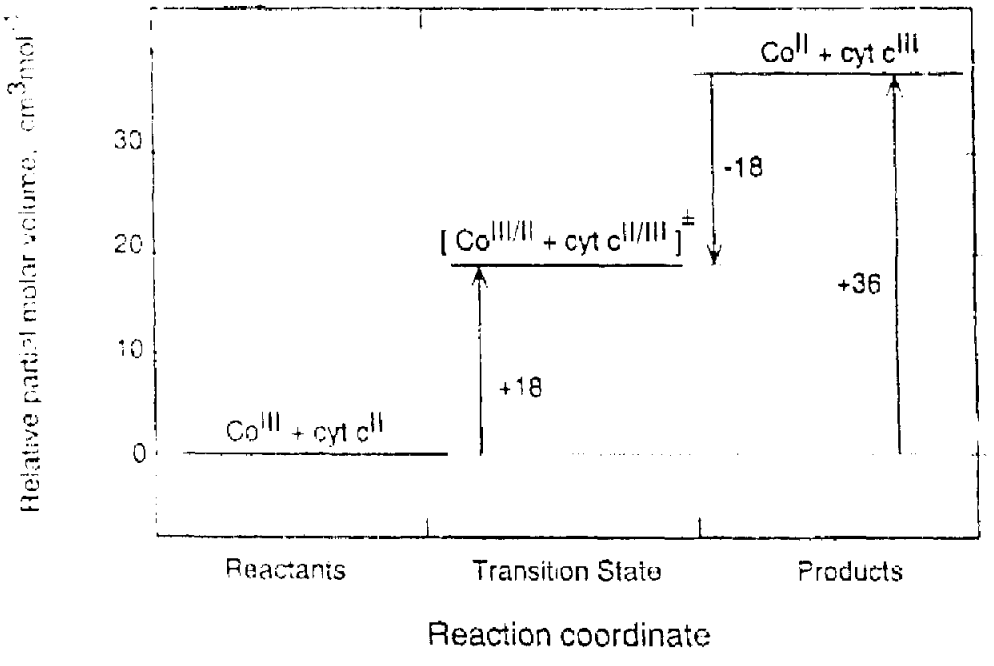

Fig. 14. Volume profile for the reversible interaction of Co(II,III)(ammines) with cyt c (II,III) at 298 K, at neutral pH [120,123].

In these systems the volume profile is controlled by effects on the redox partner of cytochrome *c*, but this does not necessarily always have to be the case. The location of the transition state on a volume basis will reveal information concerning the 'early' and 'late' nature of the transition state, as well as details on the actual electron transfer route followed.

Recent investigations on a series of intramolecular electron-transfer reactions, closely related to the series of intermolecular reactions described above, revealed non-symmetrical volume profiles [124]. Reactions of the type:

$$(NH_3)_4(L)Ru^{III}\text{-(His33)-cyt } c^{II} \Leftrightarrow (NH_3)_4(L)Ru^{II}\text{-(His33)-cyt } c^{III} \qquad (11)$$

where L = isonicotinamide, 4-ethylpyridine, 3,5-lutidine, and pyridine, all exhibit volumes of activation for the forward reaction of between +3 and +7 cm^3 mol^{-1}, compared to overall reaction volumes of between +19 and +26 cm^3 mol^{-1}. This indicates that electron transfer from Fe to Ru is characterized by an 'early' transition state in terms of volume changes along the reaction coordinate. The overall volume changes could be accounted for in terms of electrostriction effects centered around the ammine ligands on the ruthenium center. A number of possible explanations in terms of electronic and nuclear factors were offered to account for the asymmetrical nature of the volume profile.

In another system involving the oxidation of cytochrome *c* by an anionic chromium(V) oxo complex, evidence for a late product like transition state was found on the basis of the reported volume of activation [125]. This was ascribed to the effective formation of an ion-pair precursor species as a result of the interaction between the negatively charged Cr(V) complex and the positively charged surface of cytochrome *c*.

Recently, Morishima and co-workers [126] investigated the effect of pressure on electron transfer rates in zinc ruthenium modified myoglobins. The rate constant for electron transfer from photoexcited $^3ZnP^*$ to the $Ru(NH_3)_5^{3+}$ moiety of the modified protein decreased from 5×10^7 to 55 s^{-1} upon increasing the distance from 9.5 to 19.3 Å when the Ru complex is attached to His70 and His83, respectively. This decrease in the rate constant was accompanied by an increase in $\Delta V^{\neq}$ from +4 to +17 cm^3 mol^{-1}. Within the context of the results reported above and the volume changes associated with the reduction of the Ru(III) ammine complexes, the gradual increase in $\Delta V^{\neq}$ with increasing donor–acceptor distance and with decreasing rate constant could be a clear demonstration of 'early' (for the fast) and 'late' (for the slow reactions) transition states. Volume changes mainly associated with changes in electrostriction on the Ru ammine center will control the solvent reorganization and so account for the 'early' (reactant-like) and 'late' (product-like) transition states.

4.3. Photochemical electron-transfer reactions

It is reasonable to expect that photochemical electron-transfer reactions will, similar to thermal electron-transfer processes, exhibit significant pressure effects mainly associated with changes in electrostriction that accompany the electron-transfer process [12,13].

Volume changes associated with electron transfer quenching of excited $Ru(bipy)_3^{2+}$ were recently [127] obtained from time-resolved photoacoustic calorimetric studies. A volume change of $-11\ cm^3\ mol^{-1}$ was observed for electron transfer between $[Ru(bipy)_3^{2+}]^*$ and $Fe(H_2O)_6^{3+}$. This value was ascribed to solvent to solvent reorganization associated with the electron-transfer reaction. The same workers found significantly smaller volume effects for reversible electron transfer between xanthene dyes and transition metal cyanides according to the overall reaction:

$$X^* + M(CN)_6^{4-} \rightarrow X^{\cdot-} + M(CN)_6^{3-} \qquad (12)$$

corresponding to a volume contraction for electron transfer from the excited dye to the metal cyanide and to volume expansion for electron transfer from the metal cyanide to the excited dye. Here too, solvent rearrangement was suggested to account for the observed volume effects.

A number of unimolecular photoredox reactions have been studied [12,13]. A $\Delta V_R^{\neq}$ value of $+4.8\ cm^3\ mol^{-1}$ for the charge-transfer photolysis of $Co(NH_3)_5Br^{2+}$ was found and suggested the formation of a cage radical pair, $Co(II)(Br^{\bullet})$, resulting from the LMCT excited state. Dissociation of this radical pair to the reaction products was suggested to account for the increase in volume as reflected by the positive volume of activation [128].

The photolysis of $Fe(CN)_5NO^{2-}$ via MLCT excitation results in the oxidation of the metal and solvation of the NO ligand according to the reaction:

$$Fe^{II}(CN)_5NO^{2-} + S \xrightarrow{h\nu} Fe^{III}(CN)_5S^{2-} + NO \qquad (13)$$

The quantum yield for the production of $Fe(CN)_5S^{2-}$ strongly depends on the nature of the solvent, and decreases with increasing donor number and viscosity of the medium. The values of $\Delta V_R^{\neq}$ are significantly positive (see Table 5) and correlate with the fluidity of the medium, which points to the participation of a cage recombination mechanism as outlined below [129].

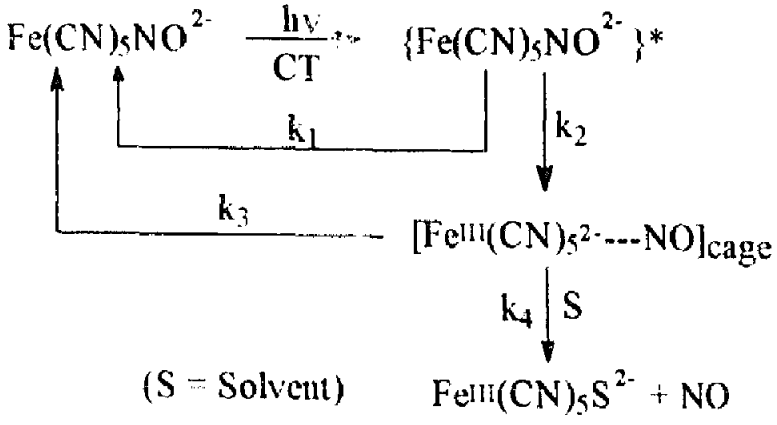

A systematic variation of the viscosity supported the validity of these arguments. The observed pressure effects in different reaction media (see Table 5),

Table 5
Values of $\Delta V_\phi^\ddagger$ and $\Delta V_\beta^\ddagger$ for the reaction: $Fe^{II}(CN)_5NO^{2-} + S \xrightarrow{h\nu} Fe^{III}(CN)_5S^{2-} + NO$ as a function of solvent and excitation energy

Solvent	λ_{irr} (nm)	ϕ [a] (mol einstein^{-1})	$\Delta V_\phi^\ddagger$ (cm^3 mol^{-1})	$\Delta V_\beta^\ddagger$ (cm^3 mol^{-1})
H_2O	436	0.17	$+7.7 \pm 0.4$	$+8.8 \pm 0.4$
	313	0.37	$+5.5 \pm 0.7$	$+7.8 \pm 1.0$
MeOH	436	0.39	$+7.2 \pm 0.5$	$+10.3 \pm 0.6$
	313	0.63	$+6.5 \pm 0.8$	$+13.0 \pm 1.9$
Me_2SO	436	0.33	$+7.9 \pm 0.3$	$+11.1 \pm 0.4$
	405	0.39	$+7.5 \pm 1.1$	$+11.4 \pm 1.6$
	313	0.42	$+8.4 \pm 1.3$	$+14.1 \pm 1.0$

[a] Values at ambient pressure, i.e. 0.1 MPa.

indicate that viscosity plays a minor role and that the effects result mainly from the contribution of k_2, that is, the dissociation of the Fe(III)–NO bond. The larger values found for $\Delta V_\beta^\ddagger$ in some of the solvents can be explained in terms of the pressure dependence of the viscosity, which will result in a decrease in ϕ and a more positive $\Delta V_\beta^\ddagger$ value (see Ref. [129] for more details).

5. Activation of small molecules

In this section we will deal with studies that involve the activation of small molecules such as O_2 and CO_2 by model coordination complexes as well as biological molecules, and focus on the mechanistic information obtained from the analysis of the corresponding volume profiles.

5.1. Activation of dioxygen

One of the most fundamental questions when dealing with the activation of dioxygen by transition metal complexes is the way in which these species really interact with each other. Are these processes controlled kinetically by substitution or by electron-transfer reactions?

In order to model the first redox activation step of dioxygen, a system that involves the binding of O_2 to a macrocyclic hexamethylcyclam Co(II) complex to form the corresponding Co(III) superoxo species, was studied [130].

$$(L)Co(H_2O)_2^{2+} + O_2 \Leftrightarrow (H_2O)(L)CoO_2^{2+} + H_2O, \quad k_1, k_{-1}, K_1 \qquad (15)$$

The overall reaction (Eq. (15)) involves ligand substitution and electron transfer to produce the Co(III) superoxo complex, the question being, which is the rate-determining step? From the pressure dependence of the overall equilibrium constant, a reaction volume of -22 cm^3 mol^{-1} was determined, which demonstrates that the displacement of a water molecule in the Co(II) complex by dioxygen is accompa-

nied by a significant volume collapse, probably due to the oxidation of Co(II) to Co(III) during the overall reaction. The kinetics of the reaction could be studied by flash photolysis, since the dioxygen complex can be photo-dissociated by irradiation into the CT band, and the subsequent reequilibration could be followed on the μs time scale. From the effect of pressure on the kinetics of binding and release of dioxygen, the activation volumes for both processes could be determined. The results show that the binding of dioxygen is accelerated by pressure, $\Delta V^{\neq}(k_1) = -4.7 \pm 0.3$ cm^3 mol^{-1}, whereas the release of dioxygen is strongly decelerated by pressure with $\Delta V^{\neq}(k_{-1}) = +17.9 \pm 0.5$ cm^3 mol^{-1}. The combination of these values yields $\Delta V(K_1) = \Delta V^{\neq}(k_1) - \Delta V^{\neq}(k_{-1}) = -22.6 \pm 0.8$ cm^3 mol^{-1}, which is in a very good agreement with the value determined directly from the equilibrium constant measurements as a function of pressure. The volume profile for this reaction is given in Fig. 15. The small volume of activation associated with the binding of dioxygen is clear evidence for a rate-limiting interchange of ligands, dioxygen for water, which is followed by an intramolecular electron-transfer reaction between Co(II) and O_2 to form $Co^{III}O_2^-$, the superoxo species. It is the latter process that accounts for the large volume collapse on the way to the reaction products, since Co(III) complexes are in general 20–30 cm^3 mol^{-1} smaller than the corresponding Co(II) complexes [103,123]. Thus, during flash-photolysis, electron transfer in the reverse direction occurs due to irradiation into the CT band, which is followed by the rapid release of dioxygen.

The binding of CO has, in many studies, been used as a model for the activation of dioxygen, since this molecule does not undergo any real activation in the systems

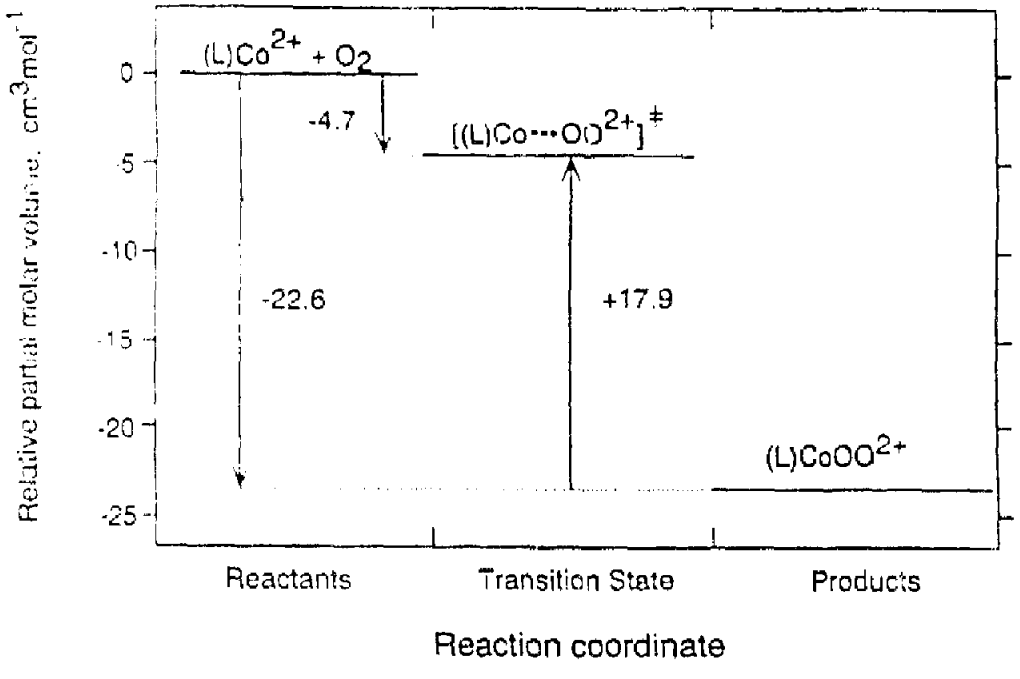

Fig. 15. Volume profile for the reaction of O_2 with the Co(III)L complex. (L = hexamethyleyclam) at 298 K [130]

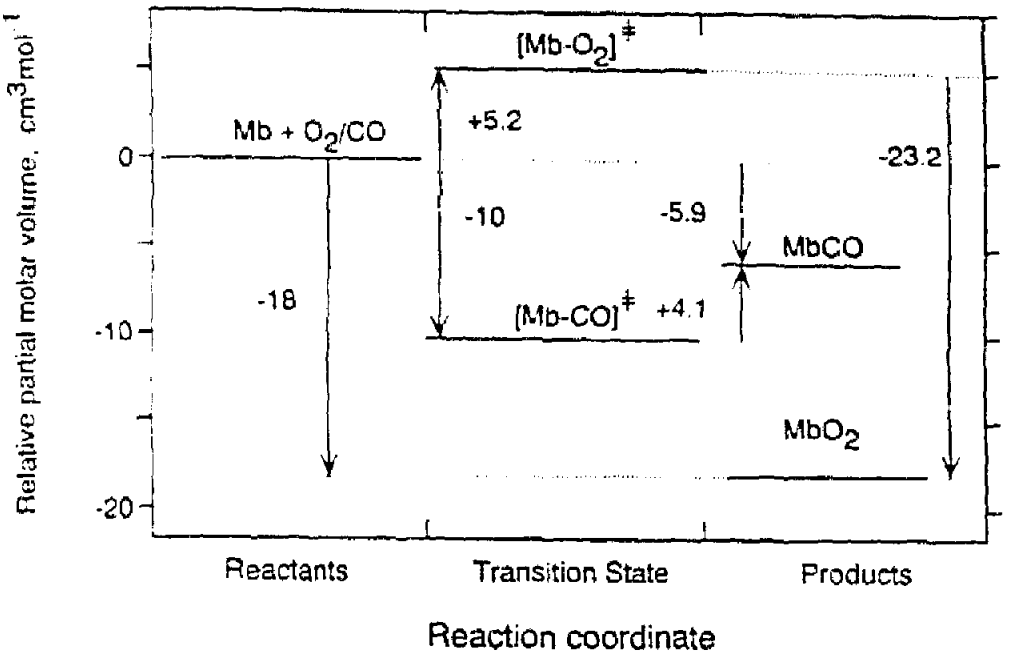

Fig. 16. Volume profile for the reactions of CO and O_2 with myoglobin at 298 K [131].

studied, it merely binds to the metal center. The absence of subsequent electron-transfer reactions simplifies the kinetic analysis and reveals more mechanistic insight on the actual binding process. A typical example concerns the comparative binding of O_2 and CO to deoxymyoglobin [131]. The large difference in $\Delta V^{\neq}$ observed for these reactions can clearly be seen from the comparative volume profiles shown in Fig. 16. The volume profile for the binding of O_2 is characterized by a substantial increase in volume on going from the reactant to the transition state, followed by a significant volume reduction on going to the product state. The observed volume increase was ascribed to rate-determining movement of O_2 through the protein to the heme pocket, which may involve hydrogen bonding to the distal histidine as well as desolvation. This step is followed by rapid bond formation with the Fe(II) center, during which the change in spin state from high to low, movement of the Fe(II) center into the porphyrin plane, and associated conformational changes account for the drastic volume reduction. The overall reaction volume of -18 cm^3 mol^{-1} demonstrates the large volume reduction caused by the binding of O_2. The volume profile for the binding of CO shows a considerable volume decrease on going from the reactant to the transition state, which has been ascribed to the rate-determining bond formation process. The reverse bond cleavage reaction is accompanied by a volume decrease, which may be related to the different bonding mode of CO compared with O_2. This difference in bonding mode must also account for the much smaller absolute reaction volume observed in this case.

The effect of pressure on the binding kinetics of O_2 and CO to myoglobin was studied in more detail on a milli-, micro-, and nanosecond time scale for sperm

whale, horse, and dog myoglobin. The results were analyzed quantitatively in terms of the following three-step mechanism:

$$A(MbL) \Leftrightarrow B(Mb, L) \Leftrightarrow C(Mb\cdots L) \Leftrightarrow S(Mb + L) \quad (16)$$

where A represents the bound species, B the short lived geminate pair, C the longer lived geminate pair, and S the entirely separated species. The volume profiles for all three myoglobins could be drawn (Fig. 17); from these it was concluded that the O_2 diffusion step within the protein matrix is quite different among the three Mb species [132]. It was further suggested that the activation volumes are very sensitive to the amino acid residues adjacent to, and flanking the ligand path channel. In the

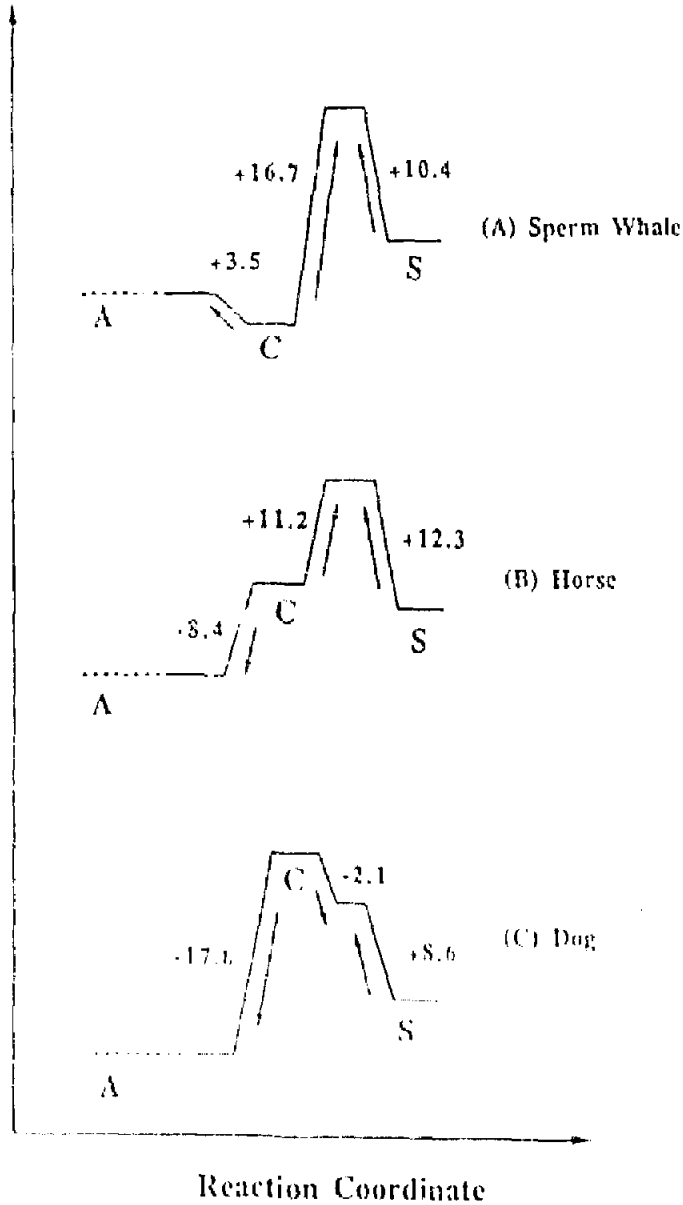

Fig. 17. Volume profiles for the binding of O_2 to different myoglobins [132].

case of CO binding [131], the overall $\Delta V^{\neq}$ was negative, which is consistent with the rate determining bond formation step.

A volume profile was also generated for the binding of dioxygen to hemerythrin [133]. The $\Delta V^{\neq}$ values for the 'on' and 'off' reactions as well as the overall reaction volume, are ca. twice the magnitude of those for the corresponding myoglobin case. In the hemerythrin system two Fe(II) centers are oxidized to Fe(III) during which dioxygen is reduced and bound as hydroperoxide to one Fe(III) center. The $\Delta V^{\neq}_{on}$ value can be partly accounted for in terms of desolvation of oxygen during its entrance into the protein. The value is however, such that it suggests some form of dynamic 'breathing' motion of the protein that momentarily causes an opening up of a cleft and enables oxygen to enter the protein. The significant volume decrease that occurs following the formation of the transition state can be ascribed to the oxidation of the Fe centers and the reduction of O_2 to O_2^-. The fact that the overall volume collapse is almost double that observed for the oxygenation of myoglobin may indicate similar structural features in oxyhemerythrin and oxymyoglobin. This would suggest that a description of the bonding mode as $Fe^{III}-O_2^-$ or $Fe^{III}-O_2H$ (H from histidine E7) instead of $Fe^{II}-O_2$, would indeed be more appropriate for oxymyoglobin.

More recently, binding of CO to lucanar Fe(II) complexes was studied in detail as a function of temperature and pressure [134,135]. In these systems the high spin Fe(II) center is five coordinate and has a vacant pocket available for the bonding of CO. These systems can therefore be considered ideal for the modeling of biological processes. A detailed kinetic analysis of the 'on' and 'off' reactions, as well as a thermodynamic analysis of the overall equilibrium, enabled the construction of free energy, entropy and volume profiles for the binding of CO to $[Fe^{II}(PhBzXy)](PF_6)$ shown in Fig. 18. The free energy profile demonstrates the favorable thermodynamic driving force for the overall reaction, as well as the relatively low activation energy for the binding process. The entropy profile demonstrates the high degree of order in the transition state on the binding of CO. The large volume collapse associated with the forward reaction is very close to the partial molar volume of CO, which suggests that CO completely disappears within the ligand pocket cavity of the complex in the transition state during partial Fe–CO bond formation. It is also known [134] that Fe–CO bond formation is accompanied by a high-spin to low-spin conversion of the Fe(II) center. In forming the six-coordinate, low-spin Fe(II) complex, the metal moves toward the plane of the equatorial nitrogen donors. Thus, following the transition state for the binding of CO, there is a high-spin to low-spin change during which bond formation is completed and the metal center moves into the ligand plane. These processes account for the subsequent volume decrease observed from the transition to the product state. The overall reaction volume of ca. -47 cm^3 mol^{-1}, therefore consists of a volume decrease of ca. -35 cm^3 mol^{-1} associated with the disappearance of CO into the ligand cavity, and ca. -12 cm^3 mol^{-1} for the high-spin to low-spin transition.

Activation of dioxygen by its interaction with copper proteins has also been studied kinetically for many model systems. Among other efforts to model the

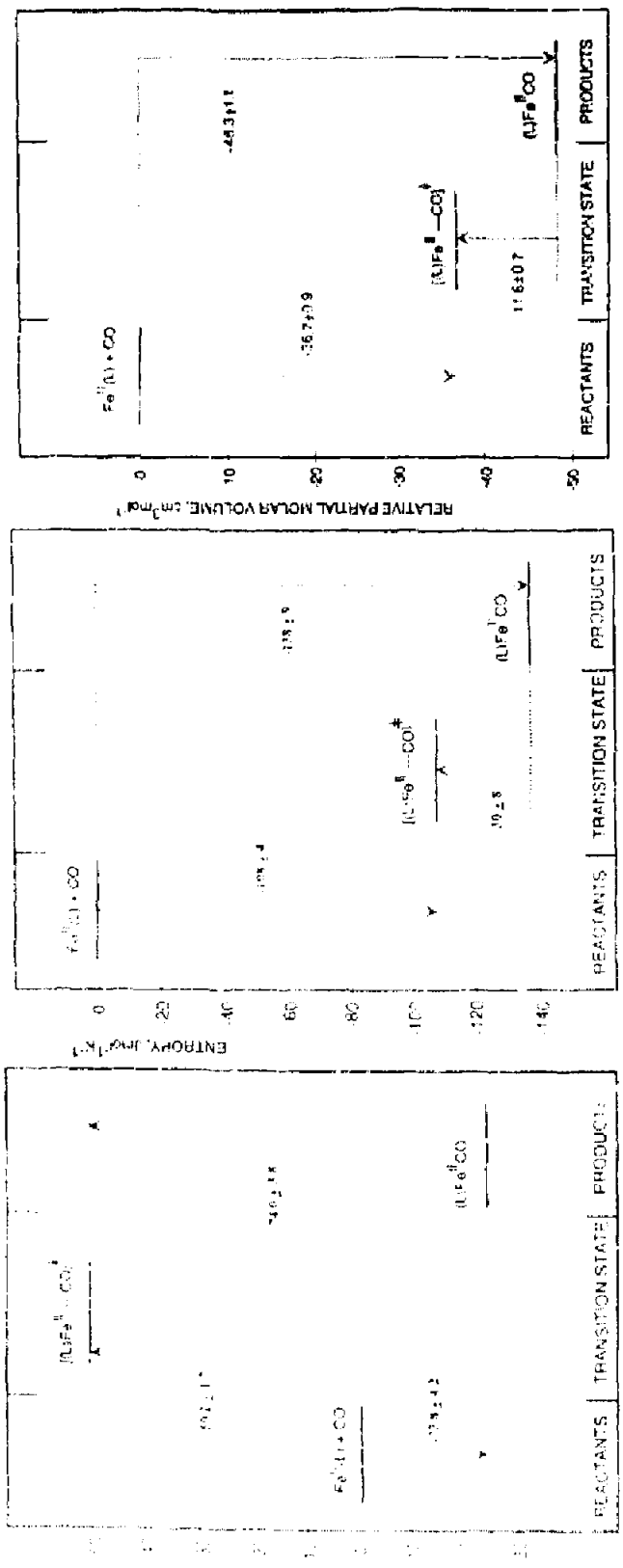

Fig. 18. Free energy and free entropy diagrams, and volume profile for the reaction of [Fe(II)(PhBAzy)(PF$_6$)] with CO in acetonitrile [134,135].

functionality of tyrosinase, a monoxygenase which activates dioxygen for *ortho* hydroxylation of monophenols, led to the development of a series of dinuclear copper model complexes [136,137]. Very detailed and sophisticated kinetic measurements have established that during the reaction of a series of dinuclear Cu(I) complexes with dioxygen, intramolecular ligand hydroxylation occurs leading to phenolate bridged Cu(II) complexes [136]. From conventional and high pressure kinetic studies on the reaction of $[Cu_2(mac)(CH_3CN)_2](PF_6)_2$ (mac = 3,6,9,17,20,23-hexatricyclo-[23.3.1.1]tiaconta-1(29),2,9,11(30),12(13),14,16,23,25,27-decaene) with dioxygen [137], the activation parameters were found to be $\Delta H^{\neq} = 32 \pm 2$ kJ mol^{-1}, $\Delta S^{\neq} = -146 \pm 8$ J K^{-1} mol^{-1} and $\Delta V^{\neq} = -21 \pm 1$ cm^3 mol^{-1}. In a rate determining step a peroxo complex is formed as an intermediate, which then reacts in a very fast reaction to give the final product. The negative $\Delta S^{\neq}$ and $\Delta V^{\neq}$ values support the idea of a highly structured transition state that is formed as a result of the presence of the highly reactive and easily oxidizable cuprous species. The negative volume of activation is a strong indication of Cu–O_2 bond formation that is accompanied by electron transfer to produce the Cu^{II}–O_2^-–Cu^{II} peroxo intermediate. The formal oxidation of Cu(I) to Cu(II) and reduction of O_2 to O_2^- are expected to be accompanied by a significant volume collapse, partly due to intrinsic and solvational volume changes. Similar results were observed for the reaction of Cu^I(phen) with dioxygen [138].

5.2. Activation of carbon dioxide

One of the most important processes dealing with the activation of CO_2 involves the hydration of CO_2 to bicarbonate, as well as the reverse dehydration of bicarbonate to produce CO_2. These processes are of biological and environmental interest since they control the transport and equilibrium behavior of CO_2. The spontaneous hydration of CO_2 and dehydration of HCO_3^- are processes that are too slow and must therefore be catalyzed by metal complexes in order to expedite the overall conversion rate.

Among others, high pressure kinetic studies on the enzymes which are efficient catalysts in biological systems have been undertaken in order to clarify the catalytic mechanism of such systems. The active center of the zinc containing metalloenzyme carbonic anhydrase (CA) consists of three histidine residues and one water molecule coordinated to zinc in a slightly distorted tetrahedral geometry. Catalytic activity is integrally related to the ionization (pK_a value ca. 7) of the coordinated water molecule, and for human CA II the mechanism is referred to as the zinc hydroxide mechanism, which has been described and modeled theoretically in considerable detail. The CA catalyzed reactions themselves have been studied in detail by many investigators using a variety of techniques, and have formed the subject of several theoretical calculations and computer simulations. The application of high pressure kinetic measurements provided further mechanistic distinction than previously available [139].

The first complete, detailed volume profile (see Fig. 19) for an enzyme catalyzed reaction in both directions has been generated [139]. The Zn(II) bound hydroxyl

moiety subjects the carbon of CO_2 to nucleophilic attack resulting in the formation of an oxygen–carbon bond, and the results are consistent with a unidentate bonding of bicarbonate. For this process the transition state lies approximately halfway between the reactant and product states (see left part of volume profile). The substitution of coordinated bicarbonate by water tends more toward a limiting D mechanism (see right part of volume profile) than would be predicted on the basis of the coordination chemistry of aquated Zn(II), which may result from the influence of the environment of the active center of the enzyme.

A wide range of methods has been used to study Co(I) complexes with tetraazamacrocyclic ligands as potential catalysts for the reduction of CO_2 [140]. The interaction of the low spin $[Co^{I}(HMD)]^{+}$ species, HMD = 5,7,7,12,14,14-hexamethyl-1,4,8,11-tetraazacyclotetradecane-4,11-diene, with CO_2 in CH_3CN leads to a five-coordinate species, $[Co(HMD)(CO_2)]^{+}$, which is in equilibrium with a six-coordinate complex ion, $[Co(HMD)(CO_2)(CH_3CN)]^{+}$, formed through addition of CH_3CN. Results from an XANES study together with other information provide a clear indication that in the six-coordinate complex cobalt is in the +3 oxidation state, meaning that the final complex ion is $Co(III)–CO_2^{-}$ (i.e. CO_2 is coordinated as carboxylate). Hence the initial Co(I) complex has reduced the bound CO_2 to carboxylate. The change in coordination number equilibrium can be studied readily by UV–vis spectrophotometry; the thermodynamic parameters are $\Delta H = -29$ kJ mol^{-1}, $\Delta S = -113$ J mol^{-1} K^{-1} and $\Delta V = -17.7$ cm^3 mol^{-1}. The latter two are mutually compatible and consistent with a highly ordered and compact six-coordinate complex ion. It has been proposed that the major part of the volume decrease arises from the intramolecular electron-transfer process accompanied by a shortening of the Co–CO_2 bond (as supported by the XANES and EXAFS studies) and an increase in electrostriction. Only a relatively minor contribution to the large negative reaction volume is suggested to result from the intrinsic effect of CH_3CN addition [140].

6. Oxidative addition and reductive elimination reactions

In general, bond formation processes are characterized by negative volumes of activation, whereas bond breakage processes are characterized by positive values. It is therefore not surprising that oxidative addition reactions are characterized by significantly negative volumes of activation, partially due to bond formation and partially due to charge creation in the transition state.

When H_2, CH_3I or HCl are added to Vaska's compound (*trans*-IrCl(CO)$(PPh_3)_2$), or related compounds, negative values of $\Delta V^{\neq}$ were found and they exhibit a meaningful solvent dependence. The variation of $\Delta V^{\neq}$ could be correlated with a polarizability function, q_p, of the solvent, permitting an extrapolation to yield a $\Delta V^{\neq}_{q_p=0}$ value of -17 to -18 cm^3 mol^{-1} [141,142]. Simultaneous formation of two Ir–H bonds to produce a *cis*-dihidrido complex upon H_2 addition was the explanation proposed, while addition of CH_3I resulted in a linear transition state, [I CH_3–IrL$_4$]. In a series of studies [143] the oxidative addition of

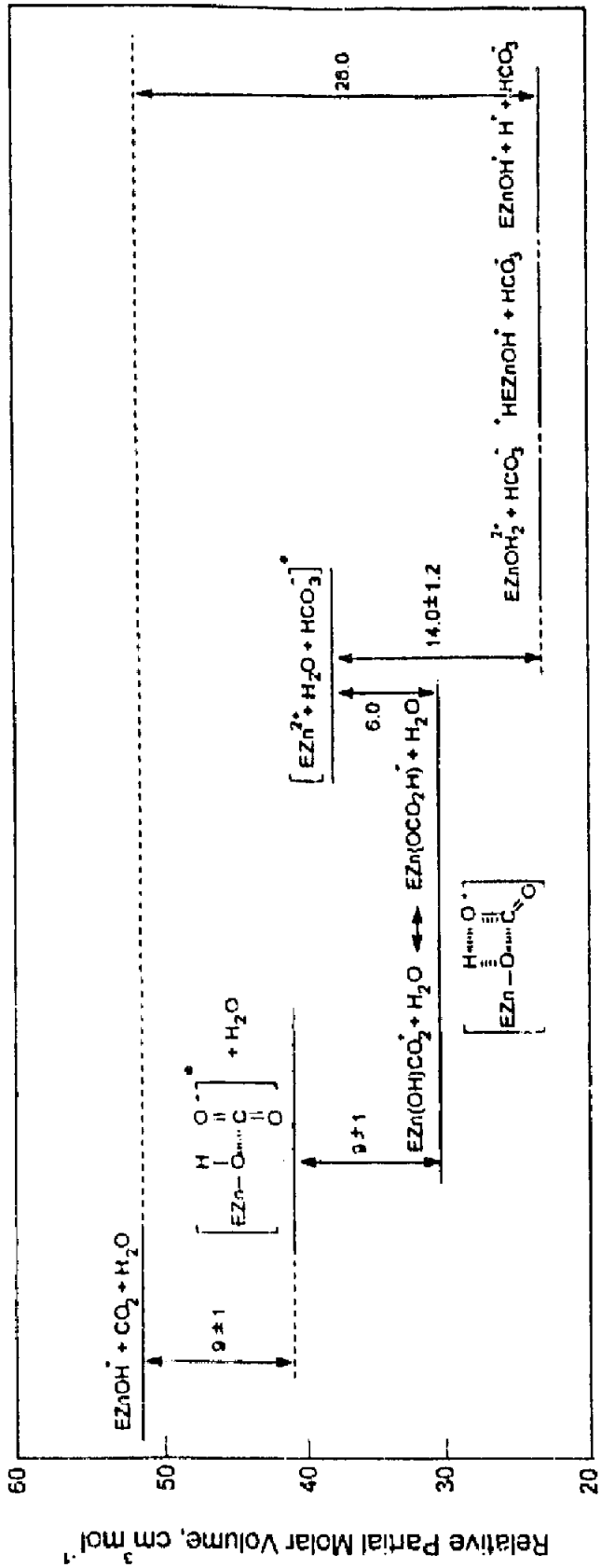

Fig. 19. Volume profile for the carbonic anhydrase catalyzed hydration of CO_2 and dehydration of HCO_3^- at 298 K [139].

iodomethane to complexes of the type Rh^{I}(β-diketonate)(CO)(PPh_3) was studied as function of pressure in different solvents. The reported volumes of activation varied between −13 and −25 cm^3 mol^{-1} and were used to describe the nature of the transition state in terms of a linear or a concerted three-center mechanism.

The kinetics of oxidative addition of CH_3I to the Pd(II) species, $PdMe_2$(bpy), to form PdIMe$_2$(bpy) in acetone have been investigated at ambient and at higher pressures [144]. A $\Delta V^{\neq}$ value of −11.9 cm^3 mol^{-1} tends to confirm the A mechanism proposed initially. The complementary reaction, reductive elimination of C_2H_6 from the Pd(IV) species, $PdIMe_3$(bpy), leaving PdIMe(bpy) likewise in acetone, was also investigated over a range of pressures. This allowed the construction of a volume profile. The latter reaction slowed down on increasing pressure, yielding a $\Delta V^{\neq}$ of +17 ± 1 cm^3 mol^{-1}, a value consistent with species production in the overall reaction, a change in the oxidation state of Pd from +IV to +II and probably considerable bond breakage in the transition state.

Elimination reactions, in general, exhibit the opposite pressure effect to those observed for oxidative addition, viz. a decrease in rate constant with increasing pressure, i.e. a positive $\Delta V^{\neq}$. In was found that the reductive elimination of hydrogen from H_2Ru_4(μ-COMe)$(CO)_{12}$ is characterized by a volume of activation of +20 ± 2 cm^3 mol^{-1}, whereas the reverse hydrogenation of HRu_4(μ-COMe)$(CO)_{12}$ is accompanied by a $\Delta V^{\neq}$ of +9.6 ± 0.6 cm^3 mol^{-1} [145].

7. Concluding remarks

The analysis of a chemical process in terms of volume changes along the reaction coordinate can help us to visualize the nature and structure of the transition state in terms of intrinsic and solvational changes in partial molar volume. With the data presently available, intrinsic volume changes are in general well understood and can be interpreted with confidence. This is, however, not the case for solvational volume changes since significantly less data are available and the interpretation is more speculative. A systematic variation of charge contributions and solvent effects have to be undertaken in order to be able to separate the intrinsic from the solvational volume contributions.

There are many cases in which it is experimentally not possible to construct a volume profile, for instance due to subsequent reactions or the irreversibility of the process as found in many electron transfer and photochemical reactions. Nevertheless, the volumes of activation for such processes can still be employed very successfully to gain further information on the nature of the transition state. As mentioned in Section 1, theoretical calculations have in recent years been successfully performed to confirm the mechanisms suggested on the basis of activation volume data and volume profile analysis, and to predict the relative size of such data. A number of important theoretical papers are cited [18,19,146–152].

It is important to realize that the presented interpretations of the $\Delta V^{\neq}$ data are all based on a simplified version of the transition state theory, which has its limitations and restrictions, and various modifications are being discussed. These

include the introduction of stochastic and transport models to account for the back-flux over the activated complex barrier in dense media [153,154]. Notwithstanding this complication, it is clear from the presentation that the additional physical parameter of pressure has not only added a decisive dimension to mechanistic studies of inorganic, organometallic and bioinorganic reactions in solution, but has also made possible the construction of reaction volume profiles that can be analyzed according to the ways demonstrated in this review.

Acknowledgements

The authors gratefully acknowledge financial support from the Alexander von Humboldt-Stiftung (GS), the Polish Research Committee, KBN, Grant T09A 115 15 (GS), the Deutsche Forschungsgemeinschaft (RvE) and the Volkswagen Foundation (RvE). They also sincerely appreciate the fine support from students and collaborators in many studies discussed in this contribution. Their names are given in the cited references.

References

[1] R. van Eldik (Ed.), Inorganic High Pressure Chemistry: Kinetics and Mechanisms, Elsevier, Amsterdam, 1986.
[2] R. van Eldik, J. Jonas (Eds.), High Pressure Chemistry and Biochemistry, Reidel, Dordrecht, 1987.
[3] R. van Eldik, C.D. Hubbard (Eds.), Chemistry under Extreme or Non-Classical Conditions, Wiley, New York, 1997.
[4] R. van Eldik, T. Asano, W.J. le Noble, Chem. Rev. 89 (1989) 549.
[5] A. Drljaca, C.D. Hubbard, R. van Eldik, T. Asano, M.V. Basilevsky, W.J. le Noble, Chem. Rev. 98 (1998) 2167.
[6] A.E. Merbach, Pure Appl. Chem. 59 (1987) 161.
[7] R. van Eldik, A.E. Merbach, Comments Inorg. Chem. 12 (1992) 341.
[8] J.W. Akitt, A.E. Merbach, NMR Basic Principles and Progress, vol. 24, Springer, Berlin, 1990, p. 189.
[9] G. Stochel, Coord. Chem. Rev. 114 (1992) 269.
[10] R. van Eldik, in: A.F. Williams, C. Floriani, A.E. Merbach (Eds.), Perspectives in Coordination Chemistry, VHCH, Basel, 1992, p. 52.
[11] G. Stochel, Coord. Chem. Rev. 159 (1997) 153.
[12] R. van Eldik, Coord. Chem. Rev. (1998), in press.
[13] R. van Eldik, P.C. Ford, in: D.C. Neckers, D.H. Volman, G. von Bunau (Eds.), Advances in Photochemistry, vol. 24, Wiley, New York, 1998, p. 61.
[14] C.D. Hubbard, R. van Eldik, Instrum. Sci. Technol. 23 (1995) 1.
[15] D. Madge, R. van Eldik, in: N. Isaacs, W. Holzapfel (Eds.), High Pressure Techniques in Chemistry and Physics: A Practical Approach, Oxford University Press, Oxford, UK, 1997, Ch. 6.
[16] T. Itoh, Y. Kitamura, K. Yoshitani, Inorg. Chem. 27 (1988) 996.
[17] Y. Ducommun, G. Laurenczy, A.E. Merbach, Inorg. Chem. 27 (1988) 1148.
[18] M. Hartmann, T. Clark, R. van Eldik, J. Am. Chem. Soc. 119 (1997) 5867.
[19] R.J. Deeth, L.J. Elding, Inorg. Chem. 35 (1996) 5019.
[20] N.J. Suvachittanont, R. van Eldik, Inorg. Chem. 28 (1989) 3660.
[21] N.J. Curtis, G.A. Lawrance, R. van Eldik, Inorg. Chem. 28 (1989) 329.

[22] G. Stochel, R. van Eldik, E. Hejmo, Z. Stasicka, Inorg. Chem. 27 (1988) 2767.
[23] G. Stochel, R. van Eldik, Inorg. Chim. Acta 155 (1989) 95.
[24] S. Alshehri, J. Burgess, Inorg. Chim. Acta 181 (1991) 153.
[25] K.B. Reddy, R. van Eldik, Inorg. Chem. 30 (1991) 596.
[26] G. Stochel, R. van Eldik, Inorg. Chim. Acta 190 (1991) 55.
[27] G. Stochel, J. Chatlas, P. Martinez, R. van Eldik, Inorg. Chem. 31 (1992) 5480.
[28] S. Alshehri, J. Burgess, R. van Eldik, C.D. Hubbard, Inorg. Chim. Acta 240 (1995) 305.
[29] I. Maciejowska, R. van Eldik, G. Stochel, Z. Stasicka, Inorg. Chem. 36 (1997) 5409.
[30] Y. Kitamura, R. van Eldik, H. Kelm, Inorg. Chem. 23 (1984) 2038.
[31] Y. Kitamura, G.A. Lawrance, R. van Eldik, Inorg. Chem. 28 (1989) 333.
[32] D.A. House, K.B. Reddy, R. van Eldik, Inorg. Chim. Acta 186 (1991) 5.
[33] P. Guardado, G.A. Lawrance, R. van Eldik, Inorg. Chem. 28 (1989) 976.
[34] M. Kotowski, R. van Eldik, in: R. van Eldik (Ed.), Inorganic High Pressure Chemistry: Kinetics and Mechanisms, Elsevier, Amsterdam, 1986, p. 219.
[35] M. Kotowski, R. van Eldik, Inorg. Chem. 25 (1986) 3896.
[36] J. Berger, M. Kotowski, R. van Eldik, U. Frey, L. Helm, A.E. Merbach, Inorg. Chem. 28 (1989) 3759.
[37] U. Frey, L. Helm, A.E. Merbach, R. Romeo, J. Am. Chem. Soc. 111 (1989) 8161.
[38] J.J. Pienaar, M. Kotowski, R. van Eldik, Inorg. Chem. 28 (1990) 373.
[39] S. Suvachittanont, H. Hohmann, R. van Eldik, J. Reedijk, Inorg. Chem. 32 (1993) 4544.
[40] Y. Koide, M. Ishikawa, K. Ishikawa, Inorg. Chim. Acta 241 (1996) 81.
[41] J-L. Jestin, J-C. Chottard, U. Frey, G. Laurenczy, A.E. Merbach, Inorg. Chem. 33 (1994) 4277.
[42] T. Rau, R. van Eldik, in: A. Sigel, H. Sigel (Eds.), Metal Ions in Biological Systems, vol. 32, Marcel Dekker, New York, 1996, p. 339.
[43] F.F. Prinsloo, J.J. Pienaar, R. van Eldik, J. Chem. Soc. Dalton Trans. (1995) 3581.
[44] H. Hohmann, B. Hellquist, R. van Eldik, Inorg. Chem. 31 (1992) 345.
[45] B.B. Hasinoff, Can. J. Chem. 52 (1974) 910.
[46] G. Stochel, R. van Eldik, H. Kunkely, A. Vogler, Inorg. Chem. 28 (1989) 4314.
[47] G. Stochel, R. van Eldik, Inorg. Chem. 29 (1990) 2075.
[48] F.F. Prinsloo, M. Meier, R. van Eldik, Inorg. Chem. 33 (1994) 900.
[49] M. Meier, R. van Eldik, Inorg. Chem. 32 (1993) 2653.
[50] F.F. Prinsloo, F.J.J. Breet, R. van Eldik, J. Chem. Soc. Dalton Trans. (1995) 685.
[51] N.F. Brasch, M.S.A. Hamza, R. van Eldik, Inorg. Chem. 36 (1997) 3216.
[52] A. Cusanelli, U. Frey, D.T. Richens, A.E. Merbach, J. Am. Chem. Soc. 118 (1996) 5265.
[53] A. Drljaca, A. Zahl, R. van Eldik, Inorg. Chem. 37 (1998) 3948.
[54] B.S. Lima Neto, D.W. Franco, R. van Eldik, J. Chem. Soc. Dalton Trans. (1995) 463.
[55] L. Dodel, H. Elias, U. Frey, A. Hörnig, U. Koelle, H. Paulus, J.S. Schneider, Inorg. Chem. 34 (1995) 306.
[56] P. Kofod, P. Harris, S. Larsen, Inorg. Chem. 36 (1997) 2258.
[57] C. Eckhard, C. Drücker-Benfer, R. van Eldik, prepared for publication.
[58] C. Ducker-Benfer, R. Dreos, R. van Eldik, Angew. Chem. Int. Ed. Engl. 34 (1995) 2245.
[59] M. Schmülling, A.D. Ryabov, R. van Eldik, J. Chem. Soc. Dalton Trans. (1994) 1257.
[60] M. Schmülling, D.M. Grove, G. van Koten, R. van Eldik, N. Veldman, A.L. Spek, Organometallics 15 (1996) 1384.
[61] R. Romeo, A. Grassi, L.M. Scolaro, Inorg. Chem. 31 (1992) 4383.
[62] D. Mannitt, J. Chem. Soc. Dalton Trans. (1993) 1343.
[63] M. Schmülling, R. van Eldik, Chem. Ber. Recueil 130 (1997) 1791.
[64] R. Romeo, M.R. Plutino, L.L. Elding, Inorg. Chem. 36 (1997) 5909.
[65] G. Laurenczy, I. Rapsport, D. Zbinden, A.E. Merbach, Magn. Res. Chem. 29 (1991) 545.
[66] M. Mizuno, S. Tanaanashi, N. Nakasuka, M. Tanaka, Inorg. Chem. 30 (1991) 1550.
[67] P.V. Bogdoon, S. Seibig, A. Zahl, R. van Eldik, prepared for publication.
[68] H.C. Bajaj, R. van Eldik, Inorg. Chem. 27 (1988) 4052.
[69] H.C. Bajaj, R. van Eldik, Inorg. Chem. 28 (1989) 1980.
[70] H.C. Bajaj, A. Das, R. van Eldik, J. Chem. Soc. Dalton Trans. (1998) 1563.

[71] D.H. Powell, P. Furrer, P.-A. Pittet, A.E. Merbach, J. Phys. Chem. 99 (1995) 16622.
[72] D.H. Powell, A.E. Merbach, I. Fabian, S. Schindler, R. van Eldik, Inorg. Chem. 33 (1994) 4468.
[73] F. Thaler, C.D. Hubbard, F. Heinemann, R. van Eldik, S. Schindler, I. Fabian, A.M. Dittler-Klingemann, F.E. Hahn, Ch. Orvig, Inorg. Chem. 37 (1998) 4022.
[74] A.M. Dittler-Klingemann, Ch. Orvig, F. Ekkehardt Hahn, F. Thaler, C.D. Hubbard, R. van Eldik, S. Schindler, I. Fabian, Inorg. Chem. 35 (1996) 7798.
[75] K. Angermann, R. van Eldik, H. Kelm, F. Wasgestian, Inorg. Chem. 20 (1981) 955.
[76] J.F. Endicott, C.K. Ryu, Comments Inorg. Chem. 6 (1[illegible]) 91.
[77] W. Weber, R. van Eldik, H. Kelm, J. Di Benedetto, Y. Du[illegible]mmun, H. Offen, P.C. Ford, Inorg. Chem. 22 (1983) 623.
[78] W. Weber, J. Di Benedetto, H. Offen, R. van Eldik, Inorg. Chem. 23 (1984) 2033.
[79] S. Wieland, R. van Eldik, J. Phys. Chem. 94 (1990) 5865.
[80] S. Wieland, R. van Eldik, J. Chem. Soc. Chem. Comm. (1989) 367.
[81] S. Wieland, K.B. Reddy, R. van Eldik, Organometallics 9 (1990) 1802.
[82] W.-F. Fu, R. van Eldik, Inorg. Chim. Acta 251 (1996) 341.
[83] W.-F. Fu, R. van Eldik, Organometallics 16 (1997) 572.
[84] W.-F. Fu, R. van Eldik, Inorg. Chem. 37 (1998) 1044.
[85] K.L. McFarlane, B. Lee, W.-F. Fu, R. van Eldik, P.C. Ford, Organometallics 17 (1998) 1826.
[86] J. Nijhoff, M.J. Bakker, T. Hartl, D.J. Stufkens, W.-F. Fu, R. van Eldik, Inorg. Chem. 37 (1998) 661.
[87] S. Zhang, V. Zang, G.R. Dobson, R. van Eldik, Inorg. Chem. 30 (1991) 355.
[88] S. Zhang, V. Zang, H.C. Bajaj, G.R. Dobson, J. Organomet. Chem. 397 (1990) 279.
[89] K.B. Reddy, R. van Eldik, Organometallics 9 (1990) 1418.
[90] Q. Ji, E.M. Eyring, R. van Eldik, K.P. Johnston, S.R. Goates, M.L. Lee, J. Phys. Chem. 99 (1995) 13461.
[91] S. Cao, K.B. Reddy, E.M. Eyring, R. van Eldik, Organometallics 13 (1994) 91.
[92] Q. Ji, C.R. Lloyd, E.M. Eyring, R. van Eldik, J. Phys. Chem. A 101 (1997) 243.
[93] R. van Eldik, H. Cohen, D. Meyerstein, Angew. Chem. Int. Ed. Engl. 30 (1991) 1158.
[94] R. van Eldik, W. Gaede, H. Cohen, D. Meyerstein, Inorg. Chem. 31 (1992) 3695.
[95] D.H. Powell, L. Helm, A.E. Merbach, J. Phys. Chem. 95 (1991) 9258.
[96] D.E. Cabelli, J.F. Wishart, J. Holeman, M. Meier, R. van Eldik, J. Phys. Chem. A 101 (1997) 5131.
[97] H. Cohen, R. van Eldik, M. Masarwa, D. Meyerstein, Inorg. Chim. Acta 177 (1990) 31.
[98] P. Wardman, J. Phys. Chem. Ref. Data 18 (1989) 1367.
[99] W.H. Jolley, D.R. Stranks, T.W. Swaddle, Inorg. Chem. 29 (1990) 1948.
[100] L. Spiccia, T.W. Swaddle, Inorg. Chem. 26 (1987) 2265.
[101] R.D. Shalders, T.W. Swaddle, Inorg. Chem. 34 (1995) 4815.
[102] Y. Fu, T.W. Swaddle, J. Am. Chem. Soc. 119 (1997) 7137.
[103] T.W. Swaddle, P.A. Tregloan, Coord. Chem. Rev., 187 (1999) 255.
[104] I. Krack, R. van Eldik, Inorg. Chem. 25 (1986) 1743.
[105] J.I. Sachinidis, R.D. Shalders, P.A. Tregloan, Inorg. Chem. 33 (1994) 6180.
[106] B. Bänsch, P. Martinez, D. Uribe, J. Zuluaga, R. van Eldik, Inorg. Chem. 30 (1991) 4555.
[107] M. Martinez, M.A. Pitarque, R. van Eldik, Inorg. Chim. Acta 256 (1997) 51.
[108] E. Ilkowska, R. van Eldik, G. Stochel, J. Biol. Inorg. Chem. 2 (1997) 603.
[109] N. Kagayama, M. Sekiguchi, Y. Inada, H.D. Takagi, S. Funahashi, Inorg. Chem. 33 (1994) 1881.
[110] A. Wanat, R. van Eldik, G. Stochel, J. Chem. Soc. Dalton Trans. (1998) 3497.
[111] B. Bänsch, P. Martinez, J. Zuluaga, D. Uribe, R. van Eldik, Z. Phys. Chem. 170 (1991) 59.
[112] J.I. Sachinidis, R.D. Shalders, P.A. Tregloan, J. Electroanal. Chem. Interfacial Electrochem. 327 (1992) 219.
[113] V. Zang, R. van Eldik, Inorg. Chem. 29 (1990) 1705.
[114] S. Seibig, R. van Eldik, Inorg. Chem. 36 (1997) 4113.
[115] S. Seibig, R. van Eldik, Fur. J. Inorg. Chem., in press.
[116] M. Meier, R. van Eldik, I.-J. Chang, G.A. Mines, D.S. Wuttke, J.R. Winkler, H.B. Gray, J. Am. Chem. Soc. 116 (1994) 1577.

[117] M. Meier, J. Sun, J.F. Wishart, R. van Eldik, Inorg. Chem. 35 (1996) 1564.
[118] B. Bänsch, M. Meier, P. Martinez, R. van Eldik, L. Su, J. Sun, S.S. Isied, J.F. Wishart, Inorg. Chem. 33 (1994) 4744.
[119] J.F. Wishart, R. van Eldik, J. Sun, L. Su, S.S. Isied, Inorg. Chem. 31 (1992) 3986.
[120] M. Meier, R. van Eldik, Inorg. Chim. Acta 225 (1994) 95.
[121] J.I. Sachinidis, R.D. Shalders, P.A. Tregloan, Inorg. Chem. 35 (1996) 2497.
[122] J. Sun, J.F. Wishart, R. van Eldik, R.D. Shalders, R.W. Swaddle, J. Am. Chem. Soc. 117 (1995) 2600.
[123] M. Meier, R. van Eldik, Chem. Eur. J. 3 (1997) 39.
[124] J. Sun, C. Su, M. Meier, S.S. Isied, J.F. Wishart, R. van Eldik, Inorg. Chem. 37 (1998) 6129.
[125] M. Koerner, R. van Eldik, submitted for publication.
[126] Y. Sugiyama, S. Takahashi, K. Ishimori, I. Morishima, J. Am. Chem. Soc. 119 (1997) 8592.
[127] J.L.H. Jiwan, A.K. Chibisov, S.E. Braslavsky, J. Phys. Chem. 99 (1995) 10246.
[128] A.D. Kirk, C. Namasivayam, G.B. Porter, M.A. Rampi-Scandola, A. Simmons, J. Phys. Chem. 87 (1983) 3108.
[129] G. Stochel, R. van Eldik, Z. Stasicka, Inorg. Chem. 25 (1986) 3663.
[130] M. Zhang, R. van Eldik, J.H. Espenson, A. Bakac, Inorg. Chem. 33 (1994) 130.
[131] H.-D. Projahn, R. van Eldik, Inorg. Chem. 30 (1992) 3288.
[132] S. Adachi, I. Morishima, J. Biol. Chem. 264 (1989) 18896.
[133] H.-D. Projahn, S. Schindler, R. van Eldik, D.G. Fortier, C.R. Andrew, A.G. Sykes, Inorg. Chem. 34 (1995) 5935.
[134] M. Buchalova, P.R. Warburton, R. van Eldik, D.H. Busch, J. Am. Chem. Soc. 119 (1997) 5867.
[135] M. Buchalova, D.H. Busch, R. van Eldik, Inorg. Chem. 37 (1998) 1116.
[136] K.D. Karlin, S. Kaderli, A.D. Zuberbühler, Acc. Chem. Res. 30 (1997) 139.
[137] M. Becker, S. Schindler, R. van Eldik, Inorg. Chem. 33 (1994) 5370.
[138] S. Goldstein, G. Czapski, R. van Eldik, H. Cohen, D. Meyerstein, J. Phys. Chem. 95 (1991) 1282.
[139] X. Zhang, C.D. Hubbard, R. van Eldik, J. Phys. Chem. 100 (1996) 9161.
[140] E. Fujita, R. van Eldik, Inorg. Chem. 37 (1998) 360.
[141] M. Walper, H. Kelm, Z. Phys. Chem. N. F. 113 (1978) 207.
[142] H. Kelm, H. Stieger, J. Phys. Chem. 77 (1973) 290.
[143] J.A. Venter, J.G. Leipoldt, R. van Eldik, Inorg. Chem. 30 (1991) 2207.
[144] C. Drücker-Benfer, R. van Eldik, A.J. Canty, Organometallics 13 (1994) 2412.
[145] J. Anhaus, H.C. Bajaj, R. van Eldik, L.R. Nevinger, J.B. Keister, Organometallics 8 (1989) 2903.
[146] F.P. Rotzinger, J. Am. Chem. Soc. 118 (1996) 6760.
[147] F.P. Rotzinger, J. Am. Chem. Soc. 119 (1997) 5230.
[148] Th. Kowall, F. Foglia, L. Helm, A.E. Merbach, Chem. Eur. J. 2 (1996) 285.
[149] A. Bleuzen, F. Foglia, E. Furet, L. Helm, A.E. Merbach, J. Weber, J. Am. Chem. Soc. 118 (1996) 12777.
[150] Th. Kowall, P. Caravan, H. Bourgeois, L. Helm, F.P. Rotzinger, A.E. Merbach, J. Am. Chem. Soc. 120 (1998) 6569.
[151] Y. Tsutsui, H. Wasada, S. Funahashi, Bull. Chem. Soc. Jpn. 70 (1997) 1813.
[152] Y. Tsutsui, H. Wasada, S. Funahashi, Bull. Chem. Soc. Jpn. 71 (1998) 73.
[153] J. Jonas, X. Peng, Ber. Bunsenges. Phys. Chem. 95 (1991) 343.
[154] J. Troe, Ber. Bunsenges. Phys. Chem. 95 (1991) 228.